(The text is taken from: Basic Solid State Chemistry, by Anthony R. West)

1.17 Some important structure types

a) Rock salt (NaCl), zinc blende or sphalerite (ZnS), fluorite (CaF$_2$), antifluorite (Na$_2$O)

These structures are considered together because they all have *ccp/fcc* anions and differ only in the positions of the cations. In Fig. 1.20 are shown the anions in a *fcc* unit cell with all possible O, T$_+$ and T$_-$ sites for the cations. The different structures are generated as follows:

Rock salt: O occupied; T$_+$ and T$_-$ empty
Zinc blende: T$_+$ (or T$_-$) occupied; O, T$_-$ (or T$_+$) empty
Antifluorite: T$_+$, T$_-$ occupied; O empty

Unit cells are shown in Fig. 1.24, in oblique projection (a-c) and as projections on the *ab* face of the unit cell in (d-f). Bach is described in more detail later.

A general rule regarding coordination numbers is that in any structure of formula A$_x$X$_y$, the coordination numbers of A and X must be in the ratio of *y: x*. In both rock salt and zinc blende, *x = y* and therefore, in each, anions and cations have the same coordination number.

In antifluorite, of formula A$_2$X, the coordination numbers of cation and anion must be in the ratio of 1:2. Since the cations occupy tetrahedral sites, the anion coordination number must be eight. In order to see this, it is convenient to redefine the origin of the unit cell to coincide with a cation rather than an anion. This is done by displacing the unit cell along a body diagonal by one quarter of the length of the diagonal. The cation at X in Fig. 1.24(c), with coordinates ¼ ¼ ¼, may be chosen as the new origin of the unit cell. The co-ordinates of all atoms in the new cell are given by subtracting ¼ ¼ ¼ from their coordinates in the old cell, as in the following table.
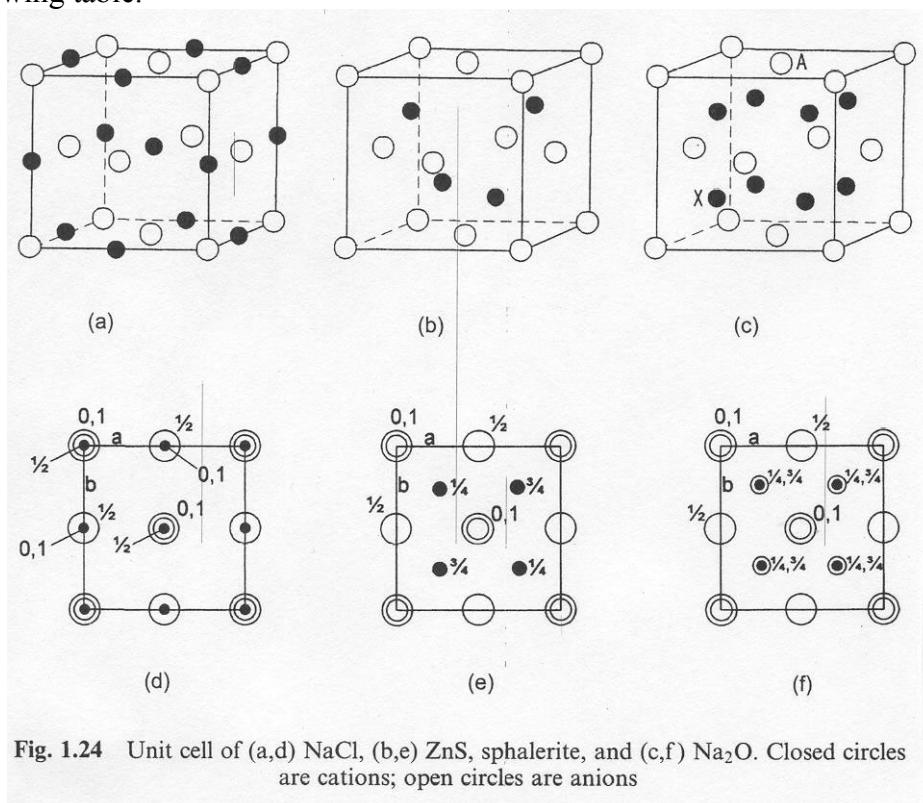

Fig. 1.24 Unit cell of (a,d) NaCl, (b,e) ZnS, sphalerite, and (c,f) Na$_2$O. Closed circles are cations; open circles are anions

	Old cell	New cell
Table 1.7	*Two ways to describe the antifluorite structure*	

	Old cell	New cell
Anions	$000, \frac{1}{2}\frac{1}{2}0, \frac{1}{2}0\frac{1}{2}, 0\frac{1}{2}\frac{1}{2}$	$\frac{3}{4}\frac{3}{4}\frac{3}{4}, \frac{1}{4}\frac{1}{4}\frac{3}{4}, \frac{1}{4}\frac{3}{4}\frac{1}{4}, \frac{3}{4}\frac{1}{4}\frac{1}{4}$
Cations	$\frac{1}{4}\frac{1}{4}\frac{1}{4}, \frac{1}{4}\frac{1}{4}\frac{3}{4}, \frac{1}{4}\frac{3}{4}\frac{1}{4}, \frac{3}{4}\frac{1}{4}\frac{1}{4}$	$000, 00\frac{1}{2}, 0\frac{1}{2}0, \frac{1}{2}00$
	$\frac{1}{4}\frac{3}{4}\frac{3}{4}, \frac{3}{4}\frac{1}{4}\frac{3}{4}, \frac{3}{4}\frac{3}{4}\frac{1}{4}, \frac{3}{4}\frac{3}{4}\frac{3}{4}$	$0\frac{1}{2}\frac{1}{2}, \frac{1}{2}0\frac{1}{2}, \frac{1}{2}\frac{1}{2}0, \frac{1}{2}\frac{1}{2}\frac{1}{2}$

In cases where negative coordinates occur as a result of this subtraction, e.g. -¼ -¼ -¼, the position lies outside the new unit cell and it is necessary to find an equivalent position within the unit cell. In this particular case, 1 is added to each coordinate, giving ¾ ¾ ¾. Addition of 1 to, say, the x coordinate is equivalent to moving to a similar position in the next unit cell in the x direction. The new unit cell of antifluorite with its origin at cation X, is shown in Fig. 1.25(a). It contains cations at corners, edge centres, face centres and body centre. In order to see the anion coordination more clearly, the unit cell may be imagined as divided into eight smaller cubes (as in Fig. 1.20). Each smaller cube has cations at all eight corners and at the centre of each is an eight-coordinate site. Anions occupy four of these eight smaller cubes such that parallel to the cell axes the eight coordinate sites are alternately occupied and empty. The eightfold coordination for one anion, A, is shown in Fig. 1.25(b).
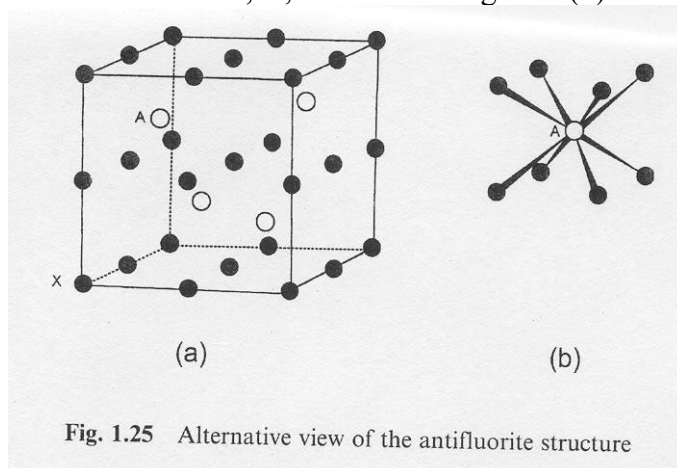

(a)   (b)

Fig. 1.25 Alternative view of the antifluorite structure

In the antifluorite structure, the effect of changing the origin from an anion to a cation is to show the structure in a completely different light. This does not happen with the rock salt and zinc blende structures. In these the cation and anion positions are interchangeable and it is immaterial whether the origin coincides with an anion or a cation.

So far the NaCl, ZnS and Na_2O structures have been described in two ways: (a) as *cp* structures; and (b) in terms of their unit cells. A third way is to regard them as built of space-filling polyhedra. Each ion and its nearest neighbours may be represented by the appropriate polyhedron, e.g. in zinc blende a tetrahedron represents one Zn with four S neighbours (or vice versa). It is then necessary to consider how neighbouring polyhedra are linked in 3D. Let us now consider each of these structures in more detail.

i) *Rock salt structure*

To summarize, the rock salt structure has *ccp/fcc* anions with octahedral sites fully occupied by cations and tetrahedral sites empty. Each cation is surrounded by six anions and similarly, each anion is octahedrally coordinated by cations (to see this, consider the anion at the body centre, 111, in Fig. 1.26; it has six cation nearest neighbours at the six face centre positions).

The ($NaCl_6$) or ($ClNa_6$) octahedra share common edges, Fig. 1.26. Since each has twelve edges and each edge is common to two octahedra it is difficult to represent this satisfactorily in a drawing; Fig. 1.26 shows two such linkages. A simplified perspective which focuses on the 3D array of octahedra is shown in Fig. 1.27; also shown, arrowed, are the empty tetrahedral sites. Each octahedron face is parallel to a *cp* layer of anions, as emphasized by the numbering or shading of coplanar faces. Parts of four different sets of faces are seen, corresponding to the four *cp* orientations in a *ccp/fcc* array.

A large number of AB compounds possess the rock salt structure. A selection is given in Table 1.7 together with values of the *a* dimension of the cubic unit cell. Most halides and hydrides of the alkali metals and Ag^+ have this structure, as do a large number of chalcogenides (oxides, sulphides, etc.) of divalent metals. Many are ionic but others are metallic, e.g. TiO, or covalent, e.g. TiC.
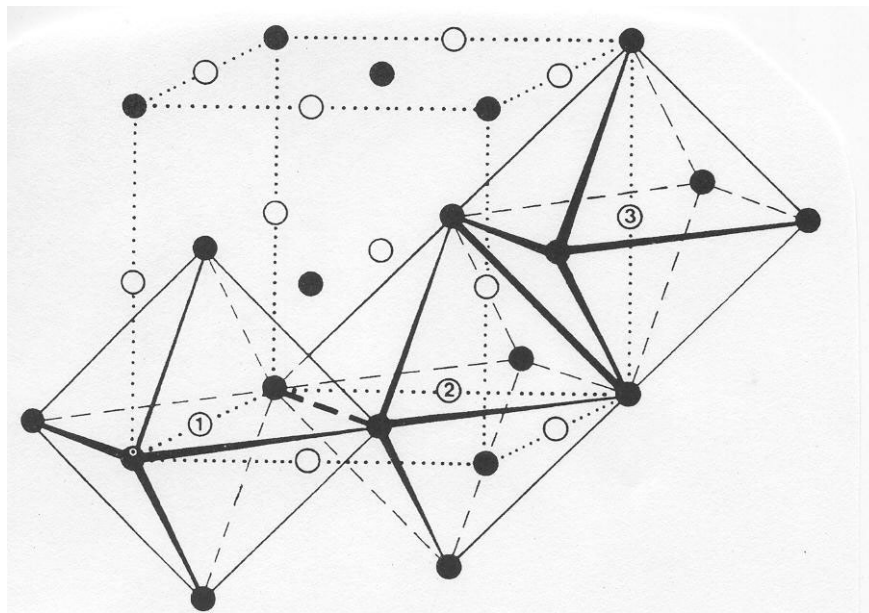

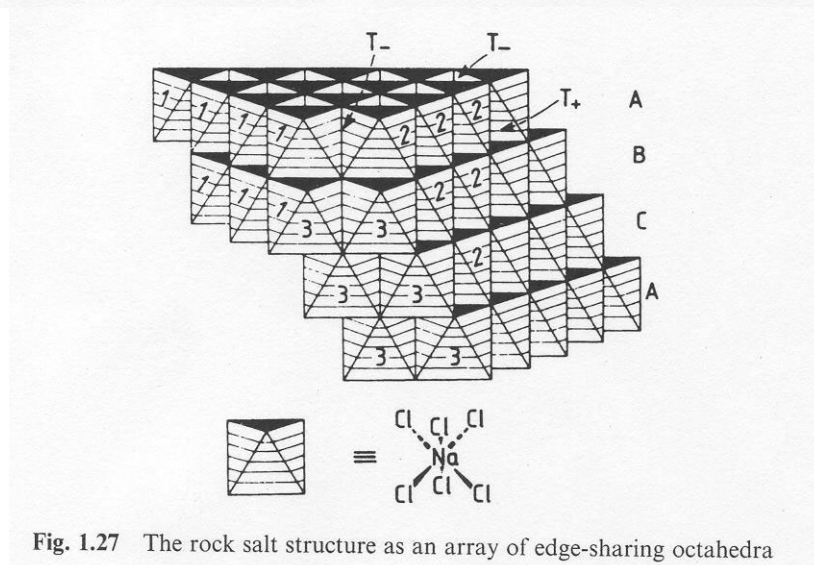**Fig. 1.26** Unit cell of the rock salt structure showing edge-sharing octahedra

Fig. 1.27 The rock salt structure as an array of edge-sharing octahedra

MgO	4.213	MgS	5.200	LiF	4.0270	KF	5.347
CaO	4.8105	CaS	5.6948	LiCl	5.1396	KCl	6.2931
SrO	5.160	SrS	6.020	LiBr	5.5013	KBr	6.5966
BaO	5.539	BaS	6.386	LiI	6.00	KI	7.0655
TiO	4.177	αMnS	5.224	LiH	4.083	RbF	5.6516
MnO	4.445	MgSe	5.462	NaF	4.64	RbCl	6.5810
FeO	4.307	CaSe	5.924	NaCl	5.6402	RbBr	6.889
CoO	4.260	SrSe	6.246	NaBr	5.9772	RbI	7.342
NiO	4.1769	BaSe	6.600	NaI	6.473	AgF	4.92
CdO	4.6953	CaTe	6.356	TiN	4.240	AgCl	5.549
TiC	4.3285	LaN	5.30	UN	4.890	AgBr	5.7745

ii) Zinc blende (sphalerite) structure

The zinc blende structure has *ccp/fcc* anions with cations in one set of tetrahedral sites, either T_+ or T_- .The ZnS_4 tetrahedra are linked at their corners and each corner is common to four such tetrahedra. The unit cell of zinc blende, Fig. 1.24(b), is shown again in Fig. 1.28(a), but in terms of corner-sharing ZnS_4 tetrahedra. The faces of the tetrahedra are parallel to the *cp* anion layers, i.e. the {111} planes; this is emphasized in a more extensive model of the structure in (b), in which the model is oriented so that one set of tetrahedron faces is approximately horizontal. Conventionally, ZnS is regarded as built of *cp* layers of sulphide anions with the smaller zinc cations in tetrahedral sites. Since the same structure is generated by interchanging the Zn and S, the structure could also be described as a *cp* array of Zn with S occupying one set of tetrahedral sites. A third, equivalent description is as an array of *ccp* ZnS_4 (or SZn_4) tetrahedra.

Some compounds with the zinc blende structure are listed in Table 1.9. The bonding is less ionic than in rock salt structure compounds. Thus, oxides do not usually have the zinc blende structure (ZnO, not included in Table 1.9, is an exception; it is dimorphic with zinc blende and wurtzite structure polymorphs). Chalcogenides of the alkaline earth metals (but not Be) have the rock salt structure whereas the chalcogenides of Be, Zn, Cd and Hg have the zinc blende structure, as do copper(I) halides and γ-AgI. A range of III-V compounds (i.e. elements from Groups III and V of the periodic table have the zinc blende structure and some, e.g. GaAs, are important semiconductors).
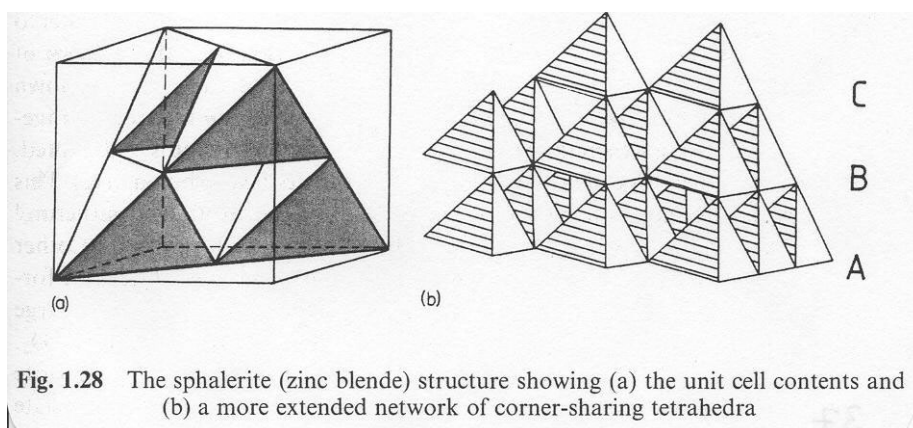

Fig. 1.28   The sphalerite (zinc blende) structure showing (a) the unit cell contents and (b) a more extended network of corner-sharing tetrahedra

Table 1.9 *Some compounds with the zinc blende (sphalerite) structure, a (Å)*

CuF	4.255	BeS	4.8624	β-CdS	5.818	BN	3.616	GaP	5.448
CuCl	5.416	BeSe	5.07	CdSe	6.077	BP	4.538	GaAs	5.6534
γ-CuBr	5.6905	BeTe	5.54	CdTe	6.481	BAs	4.777	GaSb	6.095
γ-CuI	6.051	β-ZnS	5.4060	HgS	5.8517	AlP	5.451	InP	5.869
γ-AgI	6.495	ZnSe	5.667	HgSe	6.085	AlAs	5.662	InAs	6.058
β-MnS, red	5.600	β-SiC	4.358	HgTe	6.453	AlSb	6.1347	InSb	6.4782

Elements with the diamond structure, a (Å)

C 3.5667	Si 5.4307	Ge 5.6574	α-Sn(grey) 6.4912

Table 1.10 *Some compounds with fluorite or antifluorite structure, a (Å)*

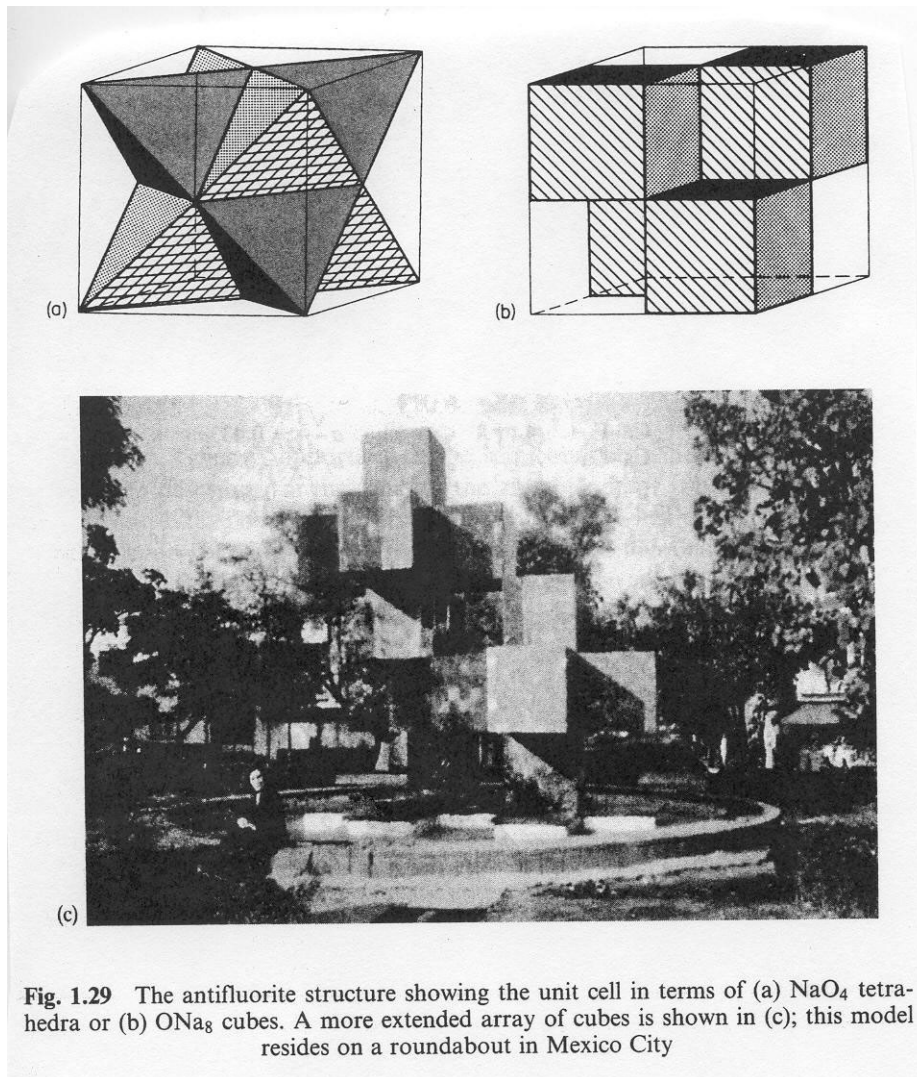| Fluorite structure				Antifluorite structure		
CaF$_2$	5.4626	PbO$_2$	5.349	Li$_2$O	4.6114	K$_2$O	6.449
SrF$_2$	5.800	CeO$_2$	5.4110	Li$_2$S	5.710	K$_2$S	7.406
SrCl$_2$	6.9767	PrO$_2$	5.392	Li$_2$Se	6.002	K$_2$Se	7.692
BaF$_2$	6.2001	ThO$_2$	5.600	Li$_2$Te	6.517	K$_2$Te	8.168
CdF$_2$	5.3895	UO$_2$	5.372	Na$_2$O	5.55	Rb$_2$O	6.74
β-PbF$_2$	5.940	NpO$_2$	5.4334	Na$_2$S	6.539	Rb$_2$S	7.65

iii) Antifluorite/fluorite structure

The antifluorite structure has *ccp/fcc* anions with cations in all (T$_+$ and T$_-$) tetrahedral sites. The difference between antifluorite and fluorite is that anti- fluorite refers to an anion array with tetrahedral cations, whereas fluorite has the inverse arrangement with a *ccp* cation array and tetrahedral anions. Since the cation: anion ratio is 2:1 in antifluorite and the cation coordination is 4, the anion coordination must be 8, Fig. 1.25.

The very different coordination environments of anions and cations leads to two entirely distinct descriptions of the structure in terms of a 3D network of either tetrahedra or cubes, Fig. 1.29; (a) corresponds to the arrangement shown in Fig. 1.24(c) and the tetrahedra are highlighted; (b) corresponds to the arrangement in Fig. 1.25(b) in which the cubic coordination arrangement is highlighted. A more extended network of corner- and edge-sharing cubes is shown in (c). This must surely rate as one of the world's largest models of the antifluorite structure!

The *antifluorite* structure is shown by a large number of oxides and other chalcogenides of the alkali metals, Table 1.10, i.e. compounds of general formula A$_2^+$X^{2-}. A group of fluorides of large, divalent cations and oxides of large tetravalent cations, have the inverse, *fluorite* structure, i.e. M^{2+}F$_2$ and M^{4+}O$_2$.

From Fig l.29(b) and (c), an alternative way of describing the fluorite structure is as a primitive cubic array of anions in which the eight-coordinate sites at the cube body centres are alternately empty and occupied by a cation. It should be stressed that the true lattice type of fluorite is *fcc* and not primitive cubic, since the primitive cubes represent only a small part (one eighth) of the *fcc* unit cell. Description of fluorite as a primitive cubic array of anions with alternate cube body centres occupied by cations shows a similarity to the CsCl structure (see later). This also has a primitive cubic array of anions, but, instead, cations occupy *all* the body centre sites.

Fig. 1.29 The antifluorite structure showing the unit cell in terms of (a) NaO_4 tetrahedra or (b) ONa_8 cubes. A more extended array of cubes is shown in (c); this model resides on a roundabout in Mexico City

iv) Bond length calculations

It is very often desirable to be able to calculate interatomic distances in crystal structures. This is usually straightforward for crystals which have *orthogonal* unit cells (i.e. $\alpha = \beta = \gamma = 90°$), and involves simple trigonometric calculations. For example, in the rock salt structure, the anion-cation distance is $a/2$ and the anion-anion distance is $a/\sqrt{2}$. The main interatomic distances involving cations in T/O sites in a *fcc/ccp* anion array are shown in Fig 1.21(c) and are summarized in Table 1.11 for the important structure types. These may be used together with the; tables of unit cell dimensions, Table 1.9, etc., for calculations on specific compounds. Typical values of bond distances (to oxygen and fluorine) for all the elements are given in Appendix 4, where relevant values for different coordination numbers and oxidation states are also given.

Table 1.11 *Calculation of interatomic distances in some simple structures*

Structure type	Distance	Number of such distances	Magnitude of distance in terms of unit cell dimensions
Rock salt (cubic)	Na–Cl	6	$a/2 = 0.5a$
	Cl–Cl	12	$a/\sqrt{2} = 0.707a$
	Na–Na	12	$a/\sqrt{2} = 0.707a$
Zinc blende (cubic)	Zn–S	4	$a\dfrac{\sqrt{3}}{4} = 0.433a$
	Zn–Zn	12	$a/\sqrt{2} = 0.707a$
	S–S	12	$a/\sqrt{2} = 0.707a$
Fluorite (cubic)	Ca–F	4 or 8	$a\dfrac{\sqrt{3}}{4} = 0.433a$
	Ca–Ca	12	$a/\sqrt{2} = 0.707a$
	F–F	6	$a/2 = 0.5a$
Wurtzite* (hexagonal)	Zn–S	4	$\dfrac{a\sqrt{3}}{8} = 0.612a = \dfrac{3c}{8} = 0.375c$
	Zn–Zn	12	$a = 0.612c$
	S–S	12	$a = 0.612c$
Nickel arsenide* (hexagonal)	Ni–As	6	$a/\sqrt{2} = 0.707a = 0.433c$
	As–As	12	$a = 0.612c$
	Ni–Ni	2	$c/2 = 0.5c = 0.816a$
	Ni–Ni	6	$a = 0.612c$
Caesium chloride (cubic)	Cs–Cl	8	$\dfrac{a\sqrt{3}}{2} = 0.866a$
	Cs–Cs	6	a
	Cl–Cl	6	a
Cadmium iodide (hexagonal)	Cd–I	6	$a/\sqrt{2} = 0.707a = 0.433c$
	I–I	12	$a = 0.612c$
	Cd–Cd	6	$a = 0.612c$

* These formulae do not necessarily apply when c/a is different from the ideal value of 1.633.

Consideration of atom arrangements in the three structure types described above shows that the concept of *cp* anions with cations in interstitial sites begins to break down in the fluorite structure. Thus, while the antifluorite structure of Na_2O may be regarded as containing *ccp* O^{2-} ions with Na^+ ions in tetrahedral sites, in the fluorite structure of CaF_2, it is necessary to regard the Ca^{2+} ions as forming the *ccp* array with F^- ions in tetrahedral sites. In CaF_2 the Ca^{2+} ions have a eutactic *ccp* arrangement, but are well separated from each other; from Tables 1.9 and 1.10, Ca-Ca = 3.86 Å, which is much larger than the diameter of a Ca^{2+} ion (depending on which table of ionic radii is consulted, the diameter of Ca^{2+} is in the range ~2.2 to 2.6 Å).

The F-F distance in CaF_2 is 2.73 Å, which indicates that the fluorines are approximately contacting $(r_{F^-} = 1.2$ to 1.4 Å). Although the array of F^- ions in CaF_2 is not *cp* but is primitive cubic, the anions are approximately in contact and this is perhaps a more realistic way of describing the structure than as containing a eutactic *ccp* array of Ca^{2+} ions.

b) Diamond

This structure type, so important to the semiconductor industry , has in fact already been described, in the form of the zinc blende or sphalerite structure, Figs 1.24 and 1.28. The diamond structure is obtained when the two elements in the zinc blende, ZnS, structure are identical, as in C. The diamond structure may therefore be described as a *ccp* array of carbon atoms, with one set of tetrahedral sites (either T_+ or T_-) occupied also by carbon atoms. It is, however, rather artificial to make a distinction between packing and interstitial atoms since

structurally they are identical. Most Group IV elements crystallize with the diamond structure, Table 1.9.

c) Wurtzite (ZnS) and nickel arsenide (NiAs)

These structures have in common a *hcp* arrangement of anions and differ only in the positions of the cations, as follows:

Wurtzite: T_+ (or T_-) sites occupied; T_- (or T_+), O empty
Nickel arsenide: O sites occupied; T_+, T_- empty

These structures are the *hcp* analogues of the *ccp* sphalerite and rock salt structures, respectively. Note that there is no hexagonal equivalent of the fluorite and antifluorite structures.

Both wurtzite and nickel arsenide have hexagonal symmetry and unit cells. A unit cell containing *hcp* anions is shown in Fig. 1.30(a). It is less easy to visualize and draw on paper than a cubic cell because of the γ angle of 120°. The unit cell contains two anions, one at the origin and one inside the cell.
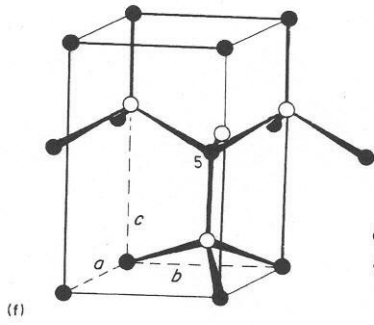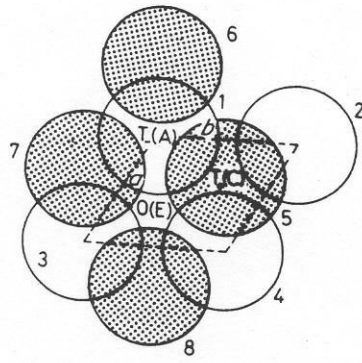
Their coordinates are:
$$(0,0,0); (1/3,2/3,1/2)$$

In Fig. 1.30(b) is shown a projection down c of the same structure. Close packed layers occur in the basal plane, i.e. at $c = 0$ (open circles), at $c = 1$ and at $c = 1/2$ (shaded circles). The layer stacking arrangement is repeated every other layer and therefore the stacking sequence is hexagonal. ..ABABA. ...Atoms 1 to 4 in the basal plane outline the base of the unit cell. The contents of one unit cell are shown in (c). Dashed circles represent atoms at the top four corners of the unit cell, i.e. at $c = 1$.
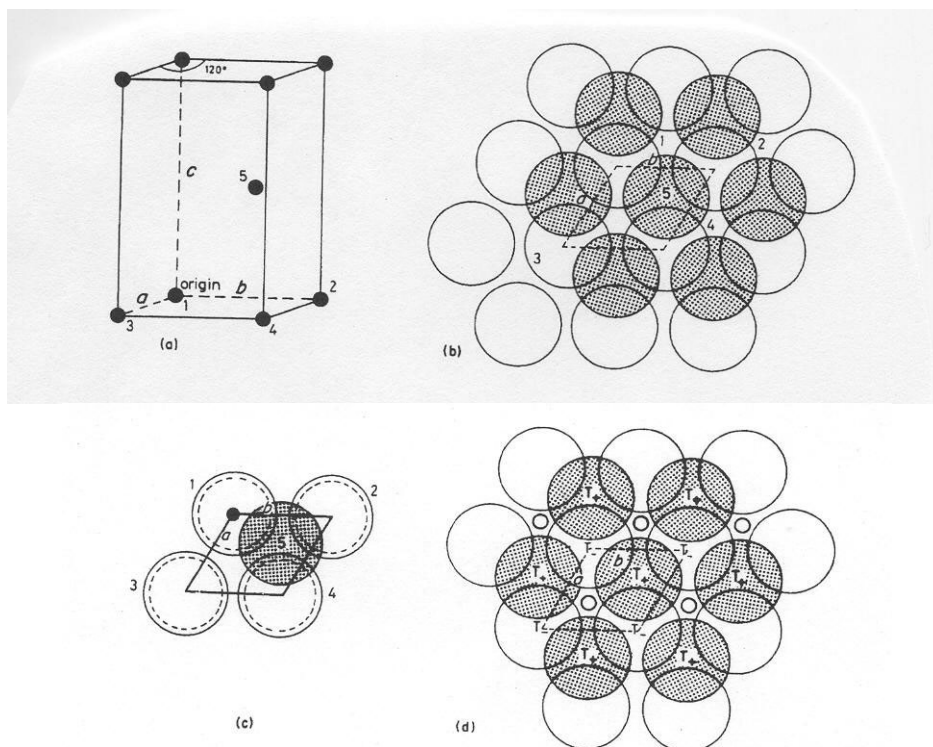
$$T_- \;:\; 0,0,\tfrac{3}{8} \;\;;\;\; \tfrac{1}{3},\tfrac{2}{3},\tfrac{7}{8}$$

$$T_+ \;:\; \tfrac{1}{3},\tfrac{2}{3},\tfrac{1}{8} \;\;;\;\; 0,0,\tfrac{5}{8}$$

$$O \;:\; \tfrac{2}{3},\tfrac{1}{3},\tfrac{1}{4} \;\;;\;\; \tfrac{2}{3},\tfrac{1}{3},\tfrac{3}{4}$$

$$\text{ANION} \;:\; 0,0,0 \;\;\;\; \tfrac{1}{3},\tfrac{2}{3},\tfrac{1}{2}$$

○ Zn
● S

(f)

(e)

○ Ni
● As

(g)

(h)

Fig. 1.30 The wurtzite and nickel arsenide structures: (a), (b), (c) the hexagonal unit cell of an *hcp* anion array; (d), (e) interstitial sites in an *hcp* array; (f), (g) structures of wurtzite and NiAs; (h), (i) trigonal prismatic coordination of arsenic in NiAs; (j), (k), (l) models of the ZnS and NiAs structures showing the arrangement and linkages of the polyhedra
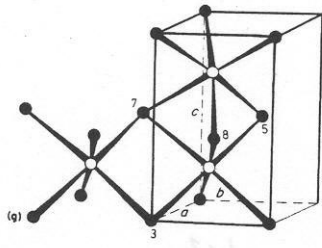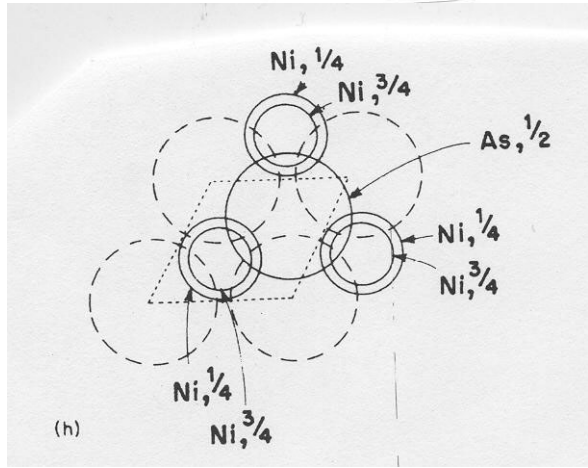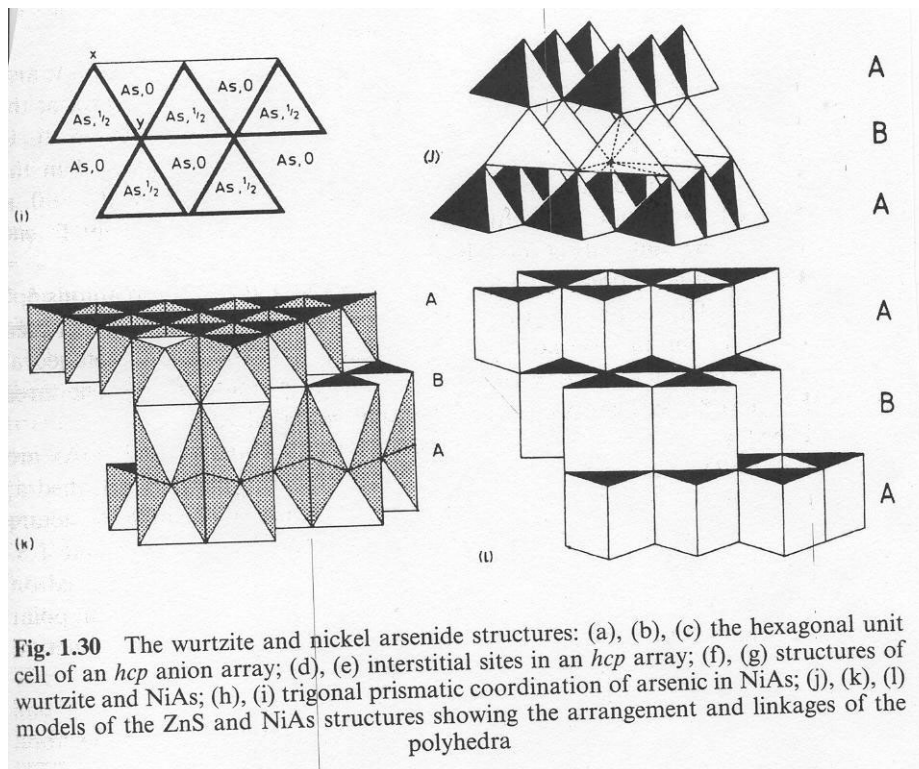
In metals which have *hcp* structures, adjacent metal atoms are in contact, e.g. 1 and 2, 1 and 4, 1 and 5 (b). In eutactic *cp* ionic structures, however, the anions may be pushed apart by the cations in the interstitial sites. Assuming for the moment that the anions are in contact, then the hexagonal unit cell has a definite shape given by the ratio $c/a = 1.633$. This is because a is equal to the shortest distance X-X, i.e. the diameter of an anion, and c is equal to twice the vertical height of a tetrahedron comprising four anions. The ratio c/a may then be calculated by geometry (Appendix 3).

The interstitial sites available for cations in a *hcp* anion array are shown in (d). Since the cell contains two anions, there must be two each of T_+, T_- and O. In (e), a T_- site, A, occurs along the c edge of the cell at height 3/8 above anion 1 at the origin. This T_- site is coordinated to three anions, shaded (5 to 7), at $c = 1/2$ and one anion (1) at the corner, $c = O$. The tetrahedron so formed therefore points downwards. The position of the T_- site inside this tetrahedron is at the centre of gravity, i.e. at one quarter of the vertical distance from base to apex (Appendix 3). Since the apex and base are at $c = 0$ and $c = 1/2$, this T_- site is at $c = 3/8$. In practice the occupant of this T_- site in the wurtzite structure may not be at exactly $0.375c$. For those structures which have been studied accurately, Table 1.11, values range from 0.345 to 0.385; the letter u represents the fractional c value.

The three anions (5 to 7) at $c = 1/2$ that form the base of this T_- site, A, also form the base of a T_+ site, B (not shown), centred at 0, 0, 5/8. The apex of the latter tetrahedron is the anion at the top corner with coordinates 0, 0, 1. Another T_+ site, C, at 1/3, 2/3, 1/8 is coordinated to anions 1, 2 and 4 in the basal plane and anion 5 at 1/3, 2/3, 1/2. The triangular base of this site, at $c = 0$, is shared with a T_- site underneath (not shown) at 1/3, 2/3, -1/8. The equivalent T_- site that lies inside the unit cell, D (not shown) is at 1/3, 2/3, 7/8.

Octahedral site E is coordinated to anions 1, 3 and 4 at $c = 0$ and anions 5, 7 and 8 at c = 1/2. The centre of gravity of the octahedron lies midway between these two groups of anions and has coordinates 2/3, 1/3, 1/4. The second octahedral site, F (not shown) lies above E at $c = 3/4$ and has coordinates 2/3, 1/3, 3/4. The three anions 5, 7 and 8 are therefore common to the two octahedra.

The coordination environments of the cations in wurtzite and NiAs are emphasized in (f) and (g). Zinc is shown in T_+ sites and forms ZnS_4 tetrahedra, (f), linked at their corners to form a 3D network, as in (j). A similar structure results on considering the tetrahedra formed by four Zn atoms around a S. The tetrahedral environment of S (5) is shown in (f). The SZn_4 tetrahedron which it forms points down, in contrast to the ZnS_4 tetrahedra which all point up; on turning the SZn_4 tetrahedra upside down, however, the same structure results.

Table 1.12   *Some compounds with the wurtzite structure* (Wyckoff, 1971, Vol. 1)

	a(Å)	c(Å)	u	c/a		a(Å)	c(Å)	u	c/a
ZnO	3.2495	5.2069	0.345	1.602	AgI	4.580	7.494		1.636
ZnS	3.811	6.234		1.636	AlN	3.111	4.978	0.385	1.600
ZnSe	3.98	6.53		1.641	GaN	3.180	5.166		1.625
ZnTe	4.27	6.99		1.637	InN	3.533	5.693		1.611
BeO	2.698	4.380	0.378	1.623	TaN	3.05	4.94		1.620
CdS	4.1348	6.7490		1.632	NH_4F	4.39	7.02	0.365	1.600
CdSe	4.30	7.02		1.633	SiC	3.076	5.048		1.641
MnS	3.976	6.432		1.618	MnSe	4.12	6.72		1.631

Comparing larger-scale models of zinc blende (Fig. 1.28b) and wurtzite (Fig. 1,30j), they are clearly very similar and both can be regarded as networks of tetrahedra. In zinc blende, layers of tetrahedra form an ABC stacking sequence and the orientation of the tetrahedra within each layer is identical. In wurtzite, the layers form an AB sequence and alternate layers are rotated by 180° about *c* relative to each other.

The $NiAs_6$ octahedra in NiAs are shown in Fig. 1.30(g). They share one pair of opposite faces (e.g. the face formed by arsenic ions 5, 7 and 8) to form chains of face-sharing octahedra that run parallel to *c*. In the *ab* plane, however, the octahedra share only edges: As atoms 3 and 7 are shared between two octahedra such that chains of edge-sharing octahedra form parallel to *b*. Similarly, chains of edge-sharing octahedra form parallel to *a* (not shown). A more extended view of the octahedra and their linkages is shown in (k).

The NiAs structure is unusual in that the anions and cations have the same coordination number but different coordination environment. Since the cation: anion ratio is l: 1 and the Ni coordination is octahedral, As must also be six coordinate. However, the six Ni neighbours are arranged as in a trigonal prism and not octahedrally. This is shown for As at $c = \frac{1}{2}$ in (h), which is coordinated to three Ni at $c = 1/4$ and three at $c = 3/4$. The two sets of Ni are superposed in projection down *c* and give trigonal prismatic coordination for As. (Note that in a similar projection for octahedral coordination, the two sets of three coordinating atoms are staggered relative to each other, as in (e) for octahedral site E.)

The NiAs structure may also be regarded as built of $AsNi_6$ trigonal prisms, therefore, which link up by sharing edges to form a 3D array. In (i) each triangle represents a prism in projection down *c*. The prism edges that run parallel to *c*, i.e. those formed by Ni at $c=1/4$ and 3/4 in (h), are shared between three prisms. Prism edges that lie in the *ab* plane are shared between only two prisms, however. In (i), the edge *xy* is shared between As at $c = 1/2$ and $c = 0$.

The structure therefore has layers of prisms arranged in an. ..ABABA. .. hexagonal stacking sequence, as shown further in (l).

A selection of compounds with wurtzite and NiAs structures is given in Tables 1.12 and 1.13 with values of their hexagonal cell parameters *a* and *c*. The wurtzite structure is formed mainly by chalcogenides of divalent metals and is a fairly ionic structure. The NiAs structure is more metallic and is adopted by a variety of intermetallic compounds and some transition metal chalcogenides (S, Se, Te). The value of the ratio *c/a* is approximately constant in the wurtzite structures but varies considerably in compounds with the NiAs 8tructure. This is

associated with the presence of metallic bonding which arises from metal-metal interactions in the *c* direction, as follows:

First consider the environment of Ni and As
Each As is surrounded by (Table 1.11):
    6 Ni in a trigonal prism at distance $0.707a$
    12 As, *hcp* arrangement, at distance a
Each Ni is surrounded by:
    6 As, octahedrally, at distance $0.707a$
    2 Ni, linearly, parallel to *c*, at distance $0.816a$ (i.e. *c/2)*
    6 Ni, hexagonally, in *ab* plane at distance a

The main effect of changing the value of the *c/a* ratio is to alter the Ni-Ni distance parallel to *c*. Thus, in FeTe, *c/a* = 1.49, and the Fe-Fe distance parallel to *c* is reduced to $0.745a$ [i.e. *c/2* = ½ (1.49a)]*,* thereby bringing these Fe atoms into close contact and increasing the metallic bonding in the *c* direction. Simple quantitative calculations of the effect of changing the *c/a* ratio are more difficult to make since it is not readily possible to distinguish between, for example, an increase in *a* and a decrease in *c,* either of which could cause the same effect on the *c/a* ratio.

Table 1.13   *Some compounds with the NiAs structure* (Wyckoff, 1971, Vol. 1)

	a(Å)	c(Å)	c/a		a(Å)	c(Å)	c/a
NiS	3.4392	5.3484	1.555	CoS	3.367	5.160	1.533
NiAs	3.602	5.009	1.391	CoSe	3.6294	5.3006	1.460
NiSb	3.94	5.14	1.305	CoTe	3.886	5.360	1.379
NiSe	3.6613	5.3562	1.463	CoSb	3.866	5.188	1.342
NiSn	4.048	5.123	1.266	CrSe	3.684	6.019	1.634
NiTe	3.957	5.354	1.353	CrTe	3.981	6.211	1.560
FeS	3.438	5.880	1.710	CrSb	4.108	5.440	1.324
FeSe	3.637	5.958	1.638	MnTe	4.1429	6.7031	1.618
FeTe	3.800	5.651	1.487	MnAs	3.710	5.691	1.534
FeSb	4.06	5.13	1.264	MnSb	4.120	5.784	1.404
δ'-NbN*	2.968	5.549	1.870	MnBi	4.30	6.12	1.423
PtB*	3.358	4.058	1.208	PtSb	4.130	5.472	1.325
PtSn	4.103	5.428	1.323	PtBi	4.315	5.490	1.272

* Anti-NiAs structure.

d) Caesium chloride (CsCl)

The unit cell of CsCl is shown in Fig. 1.31. It is a primitive cube, containing Cl at corners and Cs at the body centre, or vice versa (note that it is *not* body centred cubic since there are different ions at corner and body centre positions). The coordination numbers of both Cs and Cl are eight with interatomic distances of $0.866a$, Table 1.11. The CsCl structure is not *cp.* In a *cp* structure, each anion has twelve other anions as next nearest neighbours, which is a characteristic feature of *cp* (or eutactic *cp*) structures. In CsCl, each Cl has only six Cl⁻ ions as next nearest neighbours (arranged octahedrally). Some compounds with the CsCl structure are given in Table 1.14. They fall into two groups, halides of large monovalent elements and a variety of intermetallic compounds.

Although CsCl is not a *cp* structure, there is a link between it and the fluorite structure, which can be described as a primitive cubic array of anions with cations in *alternate* cube body centres, Fig 1.29; in CsCl, *all* body centres are occupied.
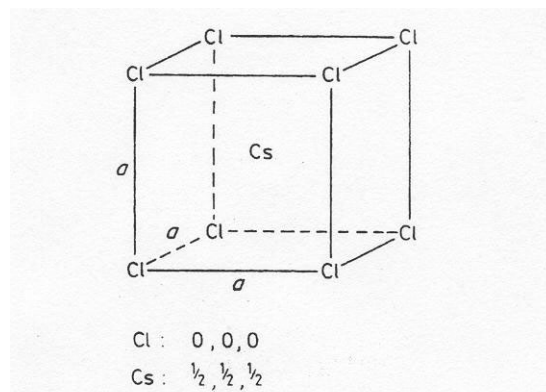
Cl : 0 , 0 , 0
Cs : $\frac{1}{2}$, $\frac{1}{2}$, $\frac{1}{2}$

Fig. 1.31   The primitive cubic unit cell of CsCl

Table 1.14   *Some compounds with the CsCl structure*

	$a(\text{Å})$		$a(\text{Å})$
CsCl	4.123	CuZn	2.945
CsBr	4.286	CuPd	2.988
CsI	4.5667	AuMg	3.259
CsCN	4.25	AuZn	3.19
NH_4Cl	3.8756	AgZn	3.156
NH_4Br	4.0594	LiAg	3.168
TlCl	3.8340	AlNi	2.881
TlBr	3.97	LiHg	3.287
TlI	4.198	MgSr	3.900

e) Other AX structures

There are five main AX structure types: rock salt, CsCl, NiAs, sphalerite and wurtzite, each of which is found in a large number of compounds. There are als0 several less common AX structures. Some are distorted variants of one of the main structure types, e.g.:

(II) FeO at low temperatures, < 90K, has a rock salt structure with a slight rhombohedral distortion (the aangle is increased from 90 to 90.07° by a slight compression along one threefold axis). This rhombohedral distortion is associated with magnetic ordering in FeO at low temperatures (Chapter 8).

(b) TlF has a rock salt related structure in which the *fcc* cell is distorted into a face centred orthorhombic cell by changing the lengths of all three cell axes by different amounts.

(c) N~CN has a distorted CsCl structure (as in NH_4Cl) in which the CN^- ions do not assume spherical symmetry but are oriented parallel to face diagonals. This distorts the symmetry to tetragonal and effectively increases *a* relative to *c*.

Other AX compounds have completely different structures, e.g.:

(a) Compounds of the d^8 ions, Pd and Pt (in PdO, PtS, etc.) often have square planar coordination for the cation; d^9 ions show this effect as well, e.g. Cu in CuO.

(b) Compounds of heavy *p*-block atoms in their lower oxidation states (e.g. Tl^+ , Pb^{2+}, Bi^{3+}) often have distorted polyhedra in which the cation exhibits the *inert pair effect.* Thus in PbO and SnO the M^{2+} ion has four O^{2-} neighbours to one side giving a square pyramidal arrangement; the O^{2-} coordination is a more regular tetrahedron of M^{2+} ions. InBi is similar with Bi^{3+} showing the inert pair effect and irregular coordination.

f) Rutile (TiO$_2$), cadmium iodide (CdI$_2$), cadmium chloride (CdCl$_2$) and caesium oxide (Cs$_2$O)

The title structures, together with fluorite, represent the main AX$_2$ structure types. The unit cell of rutile is tetragonal $a = b = 4.594$ Å, $c = 2.958$ Å, and is shown in Fig. 1.32(a). The Ti positions, two per cell, are fixed at the corner 0, 0, 0 and body centre ½ ½ ½. The O positions, four per cell, have general coordinates x,x,0; l-x,l-x,0; ½+x, ½-x, ½; ½-x, ½+x, ½, with a variable parameter, x, whose value must be determined experimentally. Crystal structure determination and refinement gave the x values listed beneath Fig. 1.32(a) for the four oxygens in the unit cell, i.e. with $x \sim 0.3$.

The body centre Ti at (½,½,½) is coordinated octahedrally to six oxygens. Four of these-two at $z = 0$ and two at 1 directly above the two at 0-are coplanar with Ti. Two oxygens at $z = $ ½ are collinear with Ti and form the axes of the octahedron. The corner Ti are also octahedrally coordinated but the orientation of their octahedra is different (b). The oxygens are coordinated trigonally to three Ti: e.g. oxygen at 0 in (a) is coordinated to Ti at the corner, at the body centre and at the body centre of .the cell below.
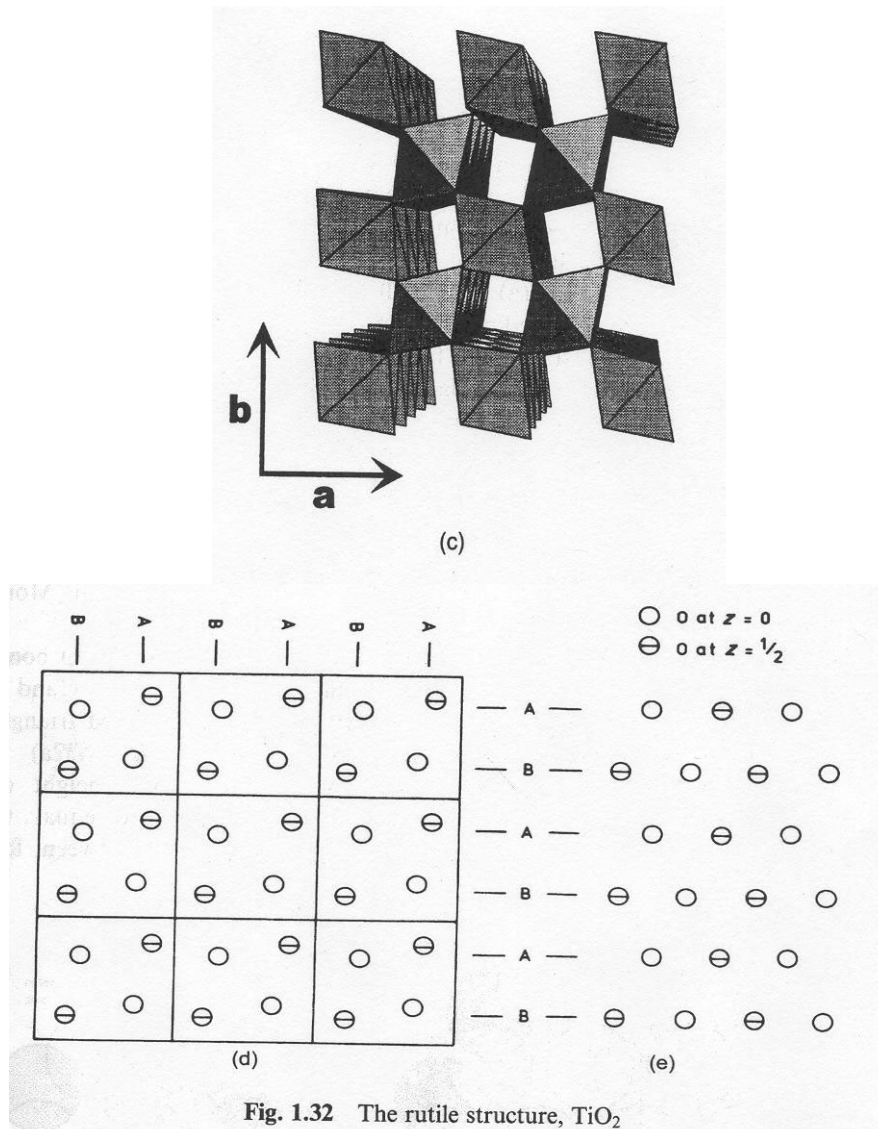

(a)   (b)

●   Ti at 000; 0.5, 0.5, 0.5

○   O at 0.3,0.3,0; 0.7,0.7,0; 0.8,0.2,0.5; 0.2,0.8,0.5
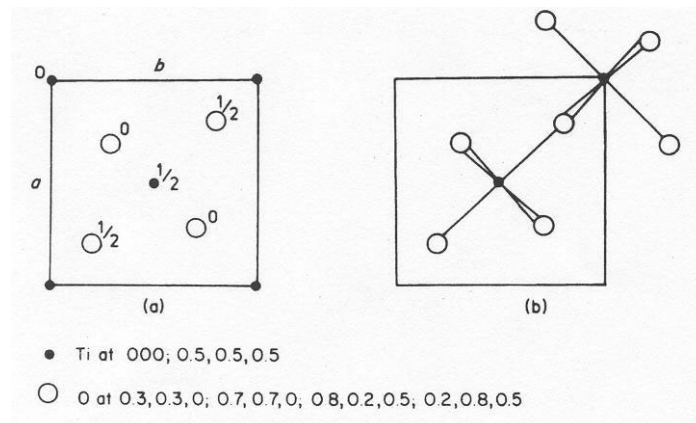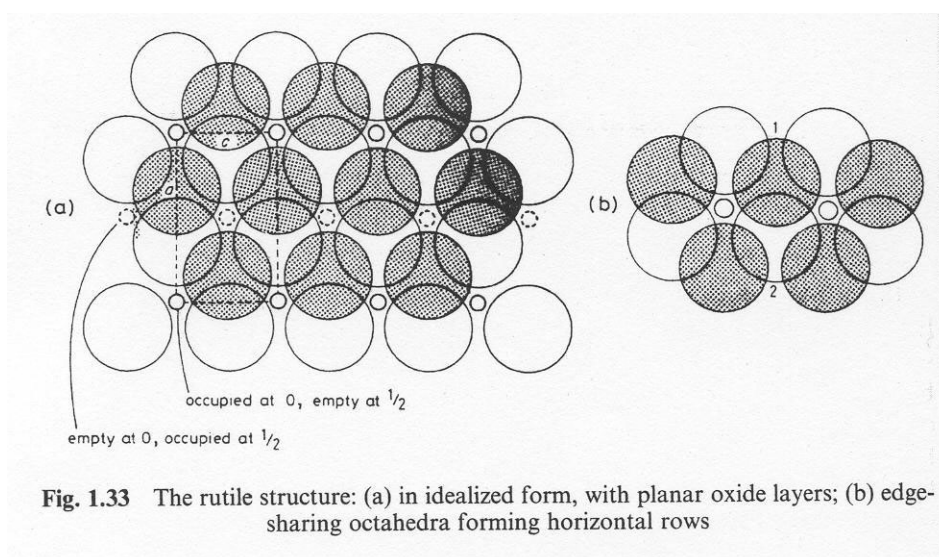
Fig. 1.32   The rutile structure, TiO_2

The TiO_6 octahedra link by sharing edges and comers to form a 3D framework. Consider the TiO_6 octahedron in the centre of the cell in (b); a similar octahedron in identical orientation occurs in the cells above and below such that octahedra in adjacent cells share edges to form infinite chains parallel to c. For example, Ti at $z = +1/2$ and $-1/2$ in adjacent cells are both coordinated to two oxygens at $z = 0$. Chains of octahedra are similarly formed by the octahedra centred at the corners of the unit cell. The two types of chains, which differ in orientation about z by 90° and which are $c/2$ out of step with each other, link by their corners to form a 3D framework (c).

The rutile structure is also commonly described as a distorted hcp oxide array with half the octahedral sites occupied by Ti. A 3x3 block of unit cells is shown in (d) with only the oxygen positions marked. Corrugated cp layers occur, both horizontally and vertically. This contrasts with the undistorted hcp arrangement (e), in which the layers occur in one orientation only (horizontally).

The octahedral sites between two cp layers in an ideal hcp anion array are shown in projection in Fig. 1.33(a). While all these sites are occupied in NiAs (Fig. 1.30h), only half are occupied in rutile and in such a manner that alternate horizontal rows of octahedral sites are full and empty. The orientation of the tetragonal unit cell in rutile is shown dashed. Parallel to the tetragonal c axis, horizontally, the TiO_6 octahedra share edges. This is shown in (b) for two octahedra with oxygens 1 and 2 forming the common edge.

15

Recently, an alternative way to describe the packing arrangement of oxide ions in rutile has been proposed. It is a slightly distorted version of a new type of packing called *primitive tetragonal packing (ptp)*, characterized by fourfold symmetry and a sphere coordination number of *eleven.* This contrasts with *hcp* and *c cp* which have a packing sphere coordination number of twelve and body centred tetragonal packing which has a coordination number of ten. More details are given in 'Further reading'.

The bond lengths in TiO$_2$ may be calculated readily; for the Ti-O bond between Ti at (1/2,1/2,1/2) and O at (0.3, 0.3, 0) the difference in both *x* and *y* parameters of Ti and O is (1/2 -0.3)a = 0.92 Å. From a right-angled triangle calculation, the Ti-O distance in projection down *c* (Fig. 1.32a) is $\sqrt{(0.92^2 + 0.92^2)}$. However, Ti and O have a difference in *c* height of (1/2-0)c = 1.48 Å and the Ti-O bond length is therefore equal to $\sqrt{(0.92^2 + 0.92^2 + 1.48^2)}$ = 1.97 Å. The axial Ti-O bond length between, for example, Ti(½, ½, ½) and O (0.8, 0.2, 0.5) is easier to calculate because both atoms are at the same *c* height. It is equal to $\sqrt{(2(0.3 \times 4.594)^2)}$ = 1.95 Å.

Fig. 1.33 The rutile structure: (a) in idealized form, with planar oxide layers; (b) edge-sharing octahedra forming horizontal rows

Two main groups of compounds exhibit the rutile structure, Table 1.15: oxides of tetravalent metals and fluorides of divalent metals. In both cases, the metals are too small to have 8-coordination and form the fluorite structure. The rutile structure may be regarded as essentially ionic.

The CdI$_2$ structure is nominally very similar to rutile because it also has an *hcp* anion array with half the octahedral sites occupied by M^{2+} ions. The manner of occupancy of the octahedral sites is quite different, however; entire layers of octahedral sites are occupied and these alternate with layers of empty cites, Fig. 1.34. CdI$_2$ is therefore a layered material in both its crystal structure And properties, in contrast to rutile which has a more rigid, 3D character.

Two I layers in a *hcp* array are shown in (a) with the octahedral sites in between occupied by Cd. To either side of the I layers, the octahedral sites are empty. Compare this with NiAs (Fig. 1.30d and h) which has the same ill1ion arrangement but with all octahedral sites occupied. The layer stacking sequence along *c* in CdI$_2$ is shown schematically in Fig. 1.34(b) and emphasizes the layered nature of the CdI$_2$ structure: I layers form an ...ABABA...stacking sequence. Cd occupies octahedral sites which may be regarded as the C positions relative to the AB positions for I. The CdI$_2$ structure may be regarded as a sandwich structure in which Cd^{2+} ions are sandwiched between layers of I$^-$ ions and adjacent sandwiches are held together by weak van der Waals bonds between the I layers. In this sense, CdI$_2$ has certain similarities to molecular structures. For example, solid CCl$_4$ has strong C-Cl bonds *within* the molecule

but only weak Cl-Cl bonds *between* adjacent molecules. Because the intermolecular forces are weak, CCl_4 is volatile with a low melting and boiling point. In the same way, CdI_2 may be regarded as an infinite sandwich 'molecule' in which there are strong Cd-I bonds within the molecule but weak van der Waals bonds between adjacent molecules.
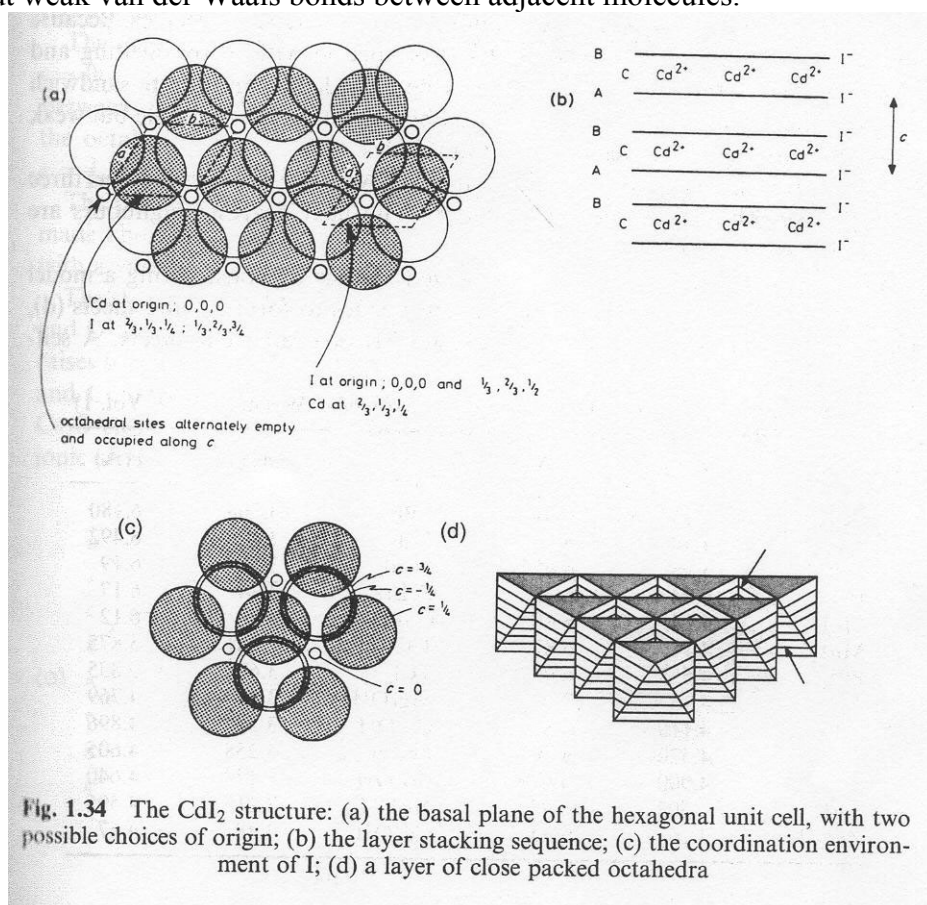

Fig. 1.34 The CdI_2 structure: (a) the basal plane of the hexagonal unit cell, with two possible choices of origin; (b) the layer stacking sequence; (c) the coordination environment of I; (d) a layer of close packed octahedra

Table 1.15   *Some compounds with the rutile structure* (Wyckoff, 1971, Vol. 1)

	a(Å)	c(Å)	x		a(Å)	c(Å)	x
TiO_2	4.5937	2.9581	0.305	CoF_2	4.6951	3.1796	0.306
CrO_2	4.41	2.91		FeF_2	4.6966	3.3091	0.300
GeO_2	4.395	2.859	0.307	MgF_2	4.623	3.052	0.303
IrO_2	4.49	3.14		MnF_2	4.8734	3.3099	0.305
β-MnO_2	4.396	2.871	0.302	NiF_2	4.6506	3.0836	0.302
MoO_2	4.86	2.79		PdF_2	4.931	3.367	
NbO_2	4.77	2.96		ZnF_2	4.7034	3.1335	0.303
OsO_2	4.51	3.19		SnO_2	4.7373	3.1864	0.307
PbO_2	4.946	3.379		TaO_2	4.709	3.065	
RuO_2	4.51	3.11		WO_2	4.86	2.77	

Table 1.16 *Some compounds with the CdI₂ structure (Wyckoff, 1971, Vol. 1)*

	$a(\text{Å})$	$c(\text{Å})$		$a(\text{Å})$	$c(\text{Å})$
CdI_2	4.24	6.84	VBr_2	3.768	6.180
CaI_2	4.48	6.96	$TiBr_2$	3.629	6.492
CoI_2	3.96	6.65	$MnBr_2$	3.82	6.19
FeI_2	4.04	6.75	$FeBr_2$	3.74	6.17
MgI_2	4.14	6.88	$CoBr_2$	3.68	6.12
MnI_2	4.16	6.82	$TiCl_2$	3.561	5.875
PbI_2	4.555	6.977	VCl_2	3.601	5.835
ThI_2	4.13	7.02	$Mg(OH)_2$	3.147	4.769
TiI_2	4.110	6.820	$Ca(OH)_2$	3.584	4.896
TmI_2	4.520	6.967	$Fe(OH)_2$	3.258	4.605
VI_2	4.000	6.670	$Co(OH)_2$	3.173	4.640
YbI_2	4.503	6.972	$Ni(OH)_2$	3.117	4.595
$ZnI_2(I)$	4.25	6.54	$Cd(OH)_2$	3.48	4.67

The coordination of I in CdI_2 is shown in (c). An I at $c = 1/4$ (shaded) has three close Cd neighbours to one side at $c = 0$. The next nearest neighbours are twelve I that form the *hcp* array.

The layered nature of CdI_2 is emphasized further by constructing a model from polyhedra: CdI_6 octahedra link at their edges to form infinite sheets (d), but there are no direct polyhedral linkages between adjacent sheets. A self supporting, 3D model of octahedra cannot be made for CdI_2, therefore. Some compounds which have the CdI_2 structure are listed in Table 1.16. It occurs mainly in transition metal iodides, bromides, chlorides and hydroxides. TiS_2 has the CdI_2 structure and was considered as a potential intercalation host cathode for use in lithium batteries (Section 7.4): Li^+ ions are able to diffuse into the empty layers that separate adjacent TiS_2 sheets at the same time that electrons can enter, and migrate through, the $3d$ band composed of d_{xy} orbitals on Ti.

The $CdCl_2$ structure is closely related to that of CdI_2 and differs only in the nature of the anion packing: Cl^- ions are *ccp* in $CdCl_2$ whereas I is *hcp* in CdI_2.

The $CdCl_2$ structure may be represented by a hexagonal unit cell, although a smaller rhombohedral cell can also be chosen. The base of the hexagonal cell is of similar size and shape to that in CdI_2 but its c axis is three times as long as c in CdI_2, This is because in $CdCl_2$, the Cd positions, and the $CdCl_6$ octahedra, are staggered along c and give rise to a three-layer repeat for Cd (CBA) and a six-layer repeat for Cl (ABCABC), Fig. 1.35. In contrast, in CdI_2, the Cd positions and the CdI_6 octahedra are stacked on top of each other and the c repeat contains only two I layers (AB) and one Cd layer (C).

The unit cell of $CdCl_2$ in projection down c is shown in (b). Cl layers occur at $c = 0$(A), 1/12 (B) and 4/12 (C) and this sequence is repeated at $c = 6/12$, 8/12 and 10/12. Between those Cl layers at 0 and 2/12 Cd occupies octahedral sites at 1/12. However, the octahedral sites between Cl layers at 2/12 and 4/12 are empty (these sites, at $c = 3/12$, are directly below Cd at 9/12),

The $CdCl_2$ structure is layered, similar to CdI_2, and many of the comments made about structure and bonding in CdI_2 apply equally well. It also occurs with a variety of transition metal halides (Table 1.17).

The structure of Cs_2O is most unusual as it is anti-$CdCl_2$. Cs forms *ccp* layers and O occupies the octahedral sites between alternate pairs of Cs layers, This raises some interesting questions because Cs is the most electropositive element and Cs salts are usually regarded as highly ionic. However, the structure of Cs_2O clearly shows that Cs is not surrounded by oxygens, as expected for an ionic structure, but has only three O neighbours, all located at one

side, The structure is held together, in three dimensions, by bonding between Cs in adjacent layers.
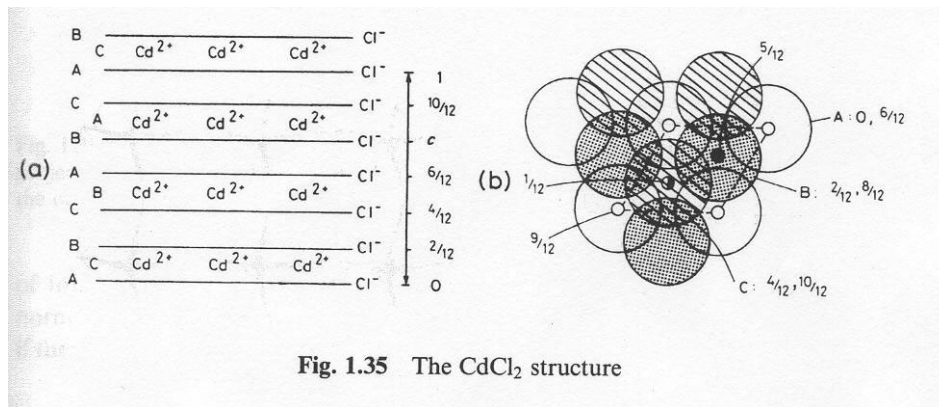

Fig. 1.35   The $CdCl_2$ structure

Table 1.17   *Some compounds with the $CdCl_2$ structure (Wyckoff, 1971, Vol. 1)*

	$a(Å)$	$c(Å)$		$a(Å)$	$c(Å)$
$CdCl_2$	3.854	17.457	$NiCl_2$	3.543	17.335
$CdBr_2$	3.95	18.67	$NiBr_2$	3.708	18.300
$CoCl_2$	3.544	17.430	NiI_2	3.892	19.634
$FeCl_2$	3.579	17.536	$ZnBr_2$	3.92	18.73
$MgCl_2$	3.596	17.589	ZnI_2	4.25	21.5
$MnCl_2$	3.686	17.470	Cs_2O^*	4.256	18.99

* Cs_2O has an anti-$CdCl_2$ structure.

It may be that the structure of Cs_2O does not reflect any peculiar type of bonding but rather that it is the only structural arrangement which is feasible for a compound of this formula and for ions of this size. Thus, from the formula, the coordination numbers of Cs and O must be in the ratio of 1:2; since Cs^+ is considerably larger than O^{2-}, the maximum possible coordination number of O by Cs may be six, which then leads to a coordination number of three for Cs.
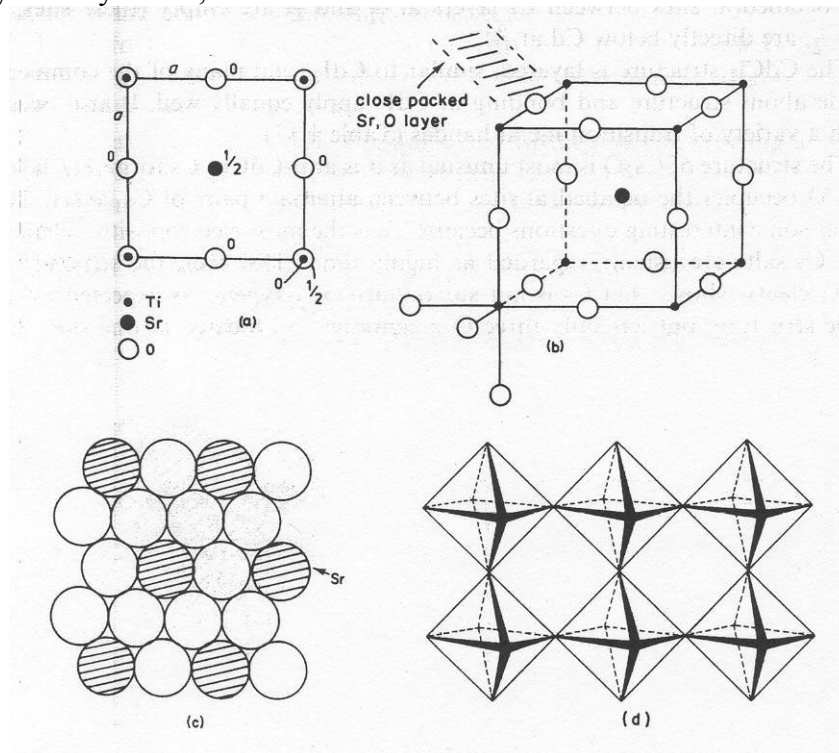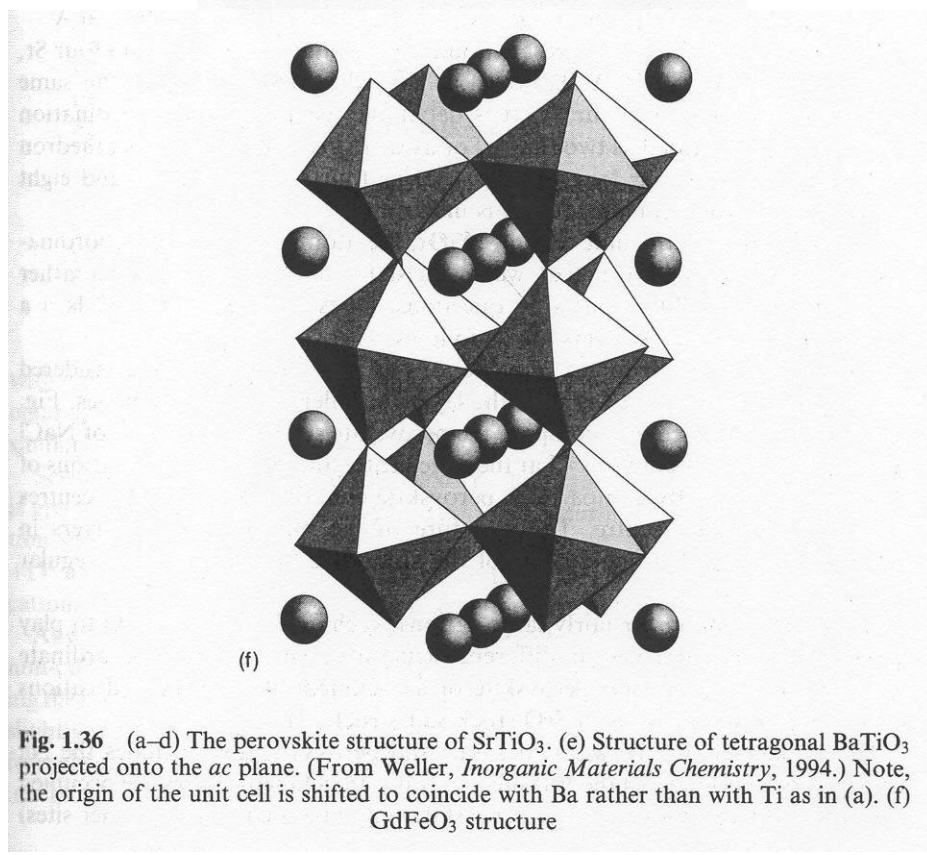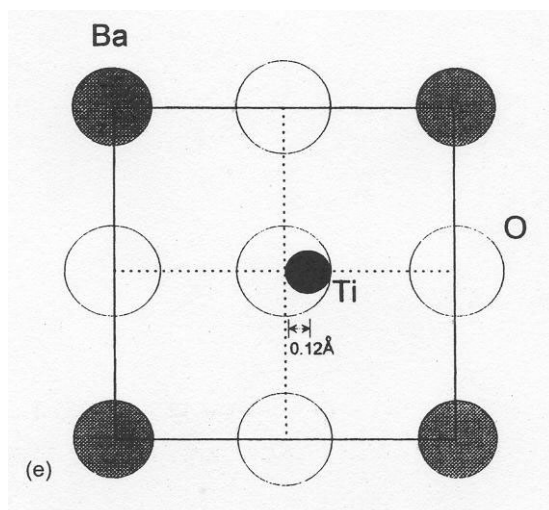
Fig. 1.36 (a–d) The perovskite structure of $SrTiO_3$. (e) Structure of tetragonal $BaTiO_3$ projected onto the *ac* plane. (From Weller, *Inorganic Materials Chemistry*, 1994.) Note, the origin of the unit cell is shifted to coincide with Ba rather than with Ti as in (a). (f) $GdFeO_3$ structure

A related question arises with the structures of the other alkali oxides, in particular K_2O and Rb_2O. These are antifluorites with coordination numbers of four and eight for M and O, respectively. These are unusual since Rb is normally far too large to enter into tetrahedral coordination with O. However, jf there is no feasible alternative structure, then perhaps Rb has no choice but to enter the tetrahedral sites. With Cs_2O, tetrahedral coordination of Cs by O is probably impossible and hence it is anti-$CdCl_2$ rather than antifluorite. Thermodynamic data qualitatively support these observations; neither Cs_2O nor Rb_2O is very stable: instead, they oxidize readily to give peroxides, M_2O_2, and superoxides, MO_2, which contain much larger anions.

g) Perovskite ($SrTiO_3$)

This very important structure type, of general formula ABX_3, has a primitive cubic unit cell, shown in Fig.1.36 as a projection down one axis (a) and as an oblique projection (b). It

contains Ti at the cube corners (coordinates 0,0,0), Sr at the body centre (1/2, 1/2, 1/2) and O at the edge centres (1/2,0,0; 0, 1/2,0; 0, 0, 1/2). The coordination environment of each atom may be seen in (b) and interatomic distances calculated by simple geometry. The octahedral coordination by oxygen of one corner Ti is shown; Ti-O $= a/2 = 1.953$ Å. Sr in the cube centre is equidistant from all twelve oxygens at edge centre positions. The Sr-O distance equals half the diagonal of any cell face, i.e. $a/\sqrt{2}$ or 2.76 Å.

Each O has two Ti as its nearest cationic neighbours, at 1.953 Å, and four Sr, coplanar with O at 2.76 Å. However, eight other oxygens are at the same distance, 2.76 Å, as the four Sr. It is debatable whether the O coordination number is best regarded as two (linear) or as six (a grossly squashed octahedron with two short and four long distances) or as fourteen (six cations and eight oxygens). No firm recommendation is made!

Having arrived at the unit cell of $SrTiO_3$, the atomic coordinates, coordination numbers and bond distances, we now wish to view the structure on a rather larger scale and ask the following questions. Does it have *cp* anions? Is it a framework structure? Answers are as follows.

Perovskite does not contain *cp* oxide ions as such but O and Sr, considered together, do form a *ccp* array with the layers parallel to the {111} planes, Fig. 1.36(b) and (c). To see this, compare the perovskite structure with that of NaCl (Fig. 1.2). The latter contains Cl at the edge centre and body centre positions of the cell and is *ccp*. By comparison, perovskite contains O at the edge centres and Sr at the body centre. The structure of the mixed Sr, O *cp* layers in perovskite is such that one quarter of the atoms are Sr, arranged in a regular fashion, Fig. 1.36(c).

It is quite common for fairly large cations, such as Sr^{2+} *(r* = 1.1 Å) to play apparently different roles in different structures, i.e. as twelve coordinate packing ions, as in $SrTiO_3$ perovskite or as octahedrally coordinated cations within a *cp* oxide array, as in SrO (rock salt structure).

The formal relation between rock salt and perovskite also includes the Na and Ti as both occupy octahedral sites: in NaCl all octahedral sites are occupied (corners and face centres), but in perovskite only one quarter (the corner sites) are occupied.

Table 1.18(a)   *Some compounds with the perovskite structure*

Compound	a(Å)	Compound	a(Å)
$KNbO_3$	4.007	$SrTiO_3$	3.9051
$KTaO_3$	3.9885	$SrZrO_3$	4.101
KIO_3	4.410	$SrHfO_3$	4.069
$NaNbO_3$	3.915	$SrSnO_3$	4.0334
$NaWO_3$	3.8622	$SrThO_3$	
$LaCoO_3$	3.824	$CsCaF_3$	4.522
$LaCrO_3$	3.874	$CsCdBr_3$	5.33
$LaFeO_3$	3.920	$CsCdCl_3$	5.20
$LaGaO_3$	3.875	$CsHgBr_3$	5.77
$LaVO_3$	3.99	$CsHgCl_3$	5.44

Table 1.18(b)   *Perovskites: some composition–property correlations*

Composition	Property
$CaTiO_3$	dielectric
$BaTiO_3$	ferroelectric
$Pb(Mg_{1/3}Nb_{2/3})O_3$	relaxor ferroelectric
$Pb(Zr_{1-x}Ti_x)O_3$	piezoelectric
$(Ba_{1-x}La_x)TiO_3$	semiconductor
$(Y_{1/3}Ba_{2/3})CuO_{3-x}$	superconductor; $O^=$ ion conductor
Na_xWO_3	mixed conductor (Na^+, e^-); electrochromic
$SrCeO_3$:H	proton conductor
RE TM O_{3-x}	mixed conductor ($O^=$, e^-)
$Li_{0.5-3x}La_{0.5+x}TiO_3$	Li^+ ion conductor
A $MnO_{3-\delta}$	giant magnetor resistance effect

Perovskite is also regarded as a framework structure with corner-sharing TiO_6 octahedra and with Sr in twelve-coordinate interstices. The octahedral coordination of one Ti is shown in (b); each O of this octahedron is shared with one other octahedron, such that the Ti-O- Ti arrangement is linear. Thus, Octahedra link at their corners to form sheets (d), and neighbouring sheets link similarly to form a 3D framework.

Several hundred oxides and halides form the perovskite structure; a selection is given in Table 1.18. The oxides contain two cations whose combined oxidation state is six. Thus, possible combinations are +I, +V as in $KNbO_3$, +II, +IV as in $CaTiO_3$ and +III, +III as in $LaGaO_3$. The 12-coordinate A site cations are, of course, much larger than the 6-coordinate B site cations.

As well as the cubic perovskite structure, described so far, a variety of distorted, non-cubic structures exist. These lower-symmetry structures often form on cooling the high-temperature cubic structures and the framework of octahedra may be slightly twisted or distorted. Some have interesting and useful properties, such as ferroelectricity (Chapter 7). In addition, more complex ordered perovskites form in which two different cations may occupy either the A or B sites.

i) Tolerance factor

The reason why structural distortions occur in many perovskites is that the A and/or B atoms are not exactly the right size to tit the sites generated by the remainder of the structure. In an oxide with the ideal, cubic perovskite structure, the bond lengths are related to the unit cell dimension, *a,* by

$$A = \sqrt{2}r_{A-O} = 2r_{B-O} \tag{1.6}$$

Since bond lengths for each element, oxidation state and coordination number usually fall within closely-defined ranges, Appendix 2, it is possible to use equation (1.6) to see how well the sizes of a particular A, B combination meet the requirements for an undistorted, ideal perovskite. The degree to which the sizes depart from equation (1.6}is given by a *tolerance factor, t*

$$t = (\sqrt{2}r_{A-O})/ (2r_{B-O}) \tag{1.7}$$

In practice, there is some flexibility over bond lengths and usually, a cubic perovskite forms with *t* in the range $0.9 < t < 1.0$.

For $t > 1$, the B site is 1arger than required. If *t* is slightly greater than 1.0, the structure distorts but is still basically a perovskite as in $BaTiO_3$, $t = 1.06$; for larger departures from $t = 1.0$, the B ion demands a smaller site, of lower coordination number and the structure changes completely, as in $BaSiO_3$ which has tetrahedral Si.

For smaller tolerance factors, $0.85 < t < 0.90$, a different kind of structural distortion occurs because now, as in GdFeO₃, the A cation is too small for its site.

For $t < 0.85$, distorted perovskite structures are no longer stable and the A cation requires a smaller site. Two examples are LiNbO₃ and ilmenite, FeTiO₃, whose structures are quite different from perovskite and in which both sets of cations are in octahedral sites (in fact, both are *hcp* structures with cations occupying 2/3 of the octahedral sites; if the two sets of cations were disordered, or indistinguishable, the structure would be that of corundum, *α*-Al₂O₃. In LiNbO₃ and FeTiO₃, the cations are ordered, but the ordering sequence is different in the two structures).

ii) BaTiO₃

BaTiO₃ is tetragonal at room temperature, $a = 3.995$, $c = 4.034$ Å with the structure shown in projection on the *ac* plane in Fig. 1.36(e). Since Ti is slightly too small for its octahedral site, it displaces by about 6% of the Ti-O distance towards one of the corner oxygens; Ba^{2+} ions also undergo a smaller displacement in the same direction. This reduces the coordination of Ti to 5 (square pyramidal) and, in order to have reasonable Ti-O bond lengths, the structure also contracts slightly in the *ab* plane [not shown in (e)].

Ti atoms in adjacent unit cells undergo a similar displacement in the same direction and the resulting structure has a large dipole moment due to the separation of positive and negative charge centres. It is possible to flip the orientation of the dipoles: under the action of an applied electric field, the Ti atoms move through the centre of the octahedral site towards one of the other corner oxygens. This ready reversibility gives the structure high polarizability and a high permittivity (or dielectric constant) and is responsible for the property of ferroelectricity (see Section 7.7).

iii) GdFeO₃

In the *GdFeO₃ structure,* the BO₆ octahedra are tilted in an alternating, zig-zag fashion (f). This has the effect of reducing the size of the A site and the coordination number is reduced from 12 to 8.

iv) Stoichiometry-property relations

The perovskite structure, with two different-sized cations and several possible cation charge combinations, occurs with a very wide range of compositions. In addition, defect perovskites form in which there are either cation or anion vacancies. Defects, solid solutions and various kinds of properties are all considered in later chapters. All we wish to note here is the incredible range of properties found in materials with perovskite-related structure whose composition has been adjusted to optimize a particular property; a selection is listed in Table 1.18(b).

h) Rhenium trioxide (ReO₃) and tungsten bronzes

These structures are closely related to perovskite described above. The cubic ReO₃ structure is the same as the 'TiO₃' framework of perovskite, SrTiO₃, but without the body centre Sr atoms. Its unit cell contains Re at comers with O at edge centres. A few oxides and halides form the ReO₃ structure, Table 1.19, together with an example of the anti-ReO₃ structure in Cu₃N.

The *tungsten bronze* structures are intermediate between ReO₃ and perovskite. They occur in the series Na$_x$WO₃ and have a 3D framework of WO₆ octahedra, as in ReO₃, but with some $(0 < x < 1)$ of the large A sites occupied by Na. To accommodate a variation in stoichiometry, *x*, the oxidation state of tungsten is a mixture of, or intermediate between, V and VI. The formula of the bronzes may be written more completely as $Na_xW_x^VW_{1-x}^{VI}O_3$.

Table 1.19 *Some compounds with the ReO₃ structure*

Compound	a(Å)	Compound	a(Å)
ReO_3	3.734	NbF_3	3.903
UO_3	4.156	TaF_3	3.9012
MoF_3	3.8985	Cu_3N	3.807

They have interesting electrical properties. At low *x,* they are pale green/yellow colour and semiconducting. As *x* rises and electrons begin to occupy the *5d* band of tungsten, they became metallic, hence the name 'bronze'.

A wide variety of monovalent cations enter the structure; similar series occur with MoO_3 in the *molybdenum bronzes*.

i) Spinel

Several commercially important magnetic oxides have the spinel structure. The parent spinel is $MgAl_2O_4$. It has *ccp* oxide ions with Mg^{2+}, Al^{3+} in tetrahedral and octahedral interstices, respectively. Many oxides, sulphides and halides have the spinel structure and different charge combinations are possible, namely:
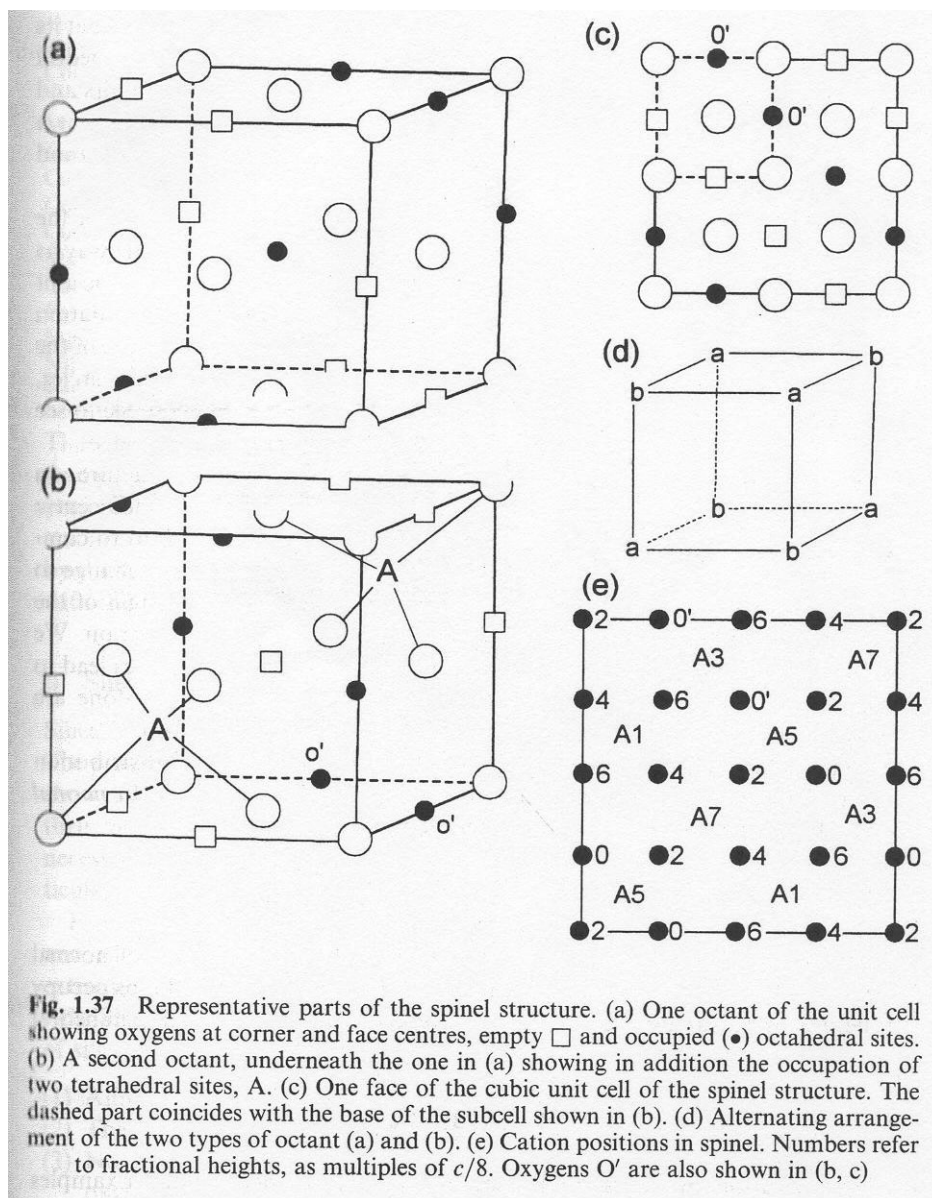
2, 3	as in	$MgAl_2O_4$
2, 4	as in	Mg_2TiO_4
1, 3, 4	as in	$LiAlTiO_4$
1, 3	as in	$Li_{0.5}Al_{2.5}O_4$
1, 2, 5	as in	$LiNiVO_4$
1, 6	as in	Na_2WO_4

Similar cation combinations occur with sulphides, e.g. 2, 3: $ZnAl_2S_4$ and 2, 4: Cu_2SnS_4. With halides, cations are limited to charges of 1 and 2, in order to give an overall cation:anion ratio of 3:4, e.g. Li_2NiF_4.

$MgAl_2O_4$ has a large, cubic unit cell with $a = 8.08$ Å. The cell contents are eight formula units (Z = 8) corresponding to '$Mg_8Al_{16}O_{32}$'. In the *ccp* oxide array, one half of the octahedral sites are occupied by Al and one eighth of the tetrahedral sites, both T_+ and T_-, by Mg. The unit cell of the spinel structure is a large cube, eight times (i.e. 2 x 2 x 2); the size of a typical face centred cube and it is almost impossible to give a comprehensible drawing of the complete unit cell and its contents. We can, however, easily understand how the structure arises and draw structural fragments to illustrate certain features.

Writing the general formula of a normal spinel as $A^{tet}B_2^{oct}O_4$, let us first consider the $B_2^{oct}O_4$ part. Quite simply, this is the rock salt structure with *ccp* O^{2-} ions but with only alternate octahedral sites occupied by B cations. Two such rock salt-derivative subcells are shown in Fig. 1.37 (a, b) (each subcell forms one octant of the spinel unit cell); the bottom face of the subcell in (a) is the same as the top face of the subcell in (b). Oxygens are shown at comers and face centres (as in Fig. 1.20). Some octahedral positions are shown as occupied (solid circles) but alternate ones in any of the three unit cell directions are empty (small squares).

The base of the spinel unit cell is shown in (c); it is formed by the base of (b), dashed, and that of three adjacent subcells. The alternating, empty-occupied- empty sequence of octahedral sites is clearly seen and also occurs similarly in the third dimension (a, b).

Fig. 1.37 Representative parts of the spinel structure. (a) One octant of the unit cell showing oxygens at corner and face centres, empty □ and occupied (•) octahedral sites. (b) A second octant, underneath the one in (a) showing in addition the occupation of two tetrahedral sites, A. (c) One face of the cubic unit cell of the spinel structure. The dashed part coincides with the base of the subcell shown in (b). (d) Alternating arrangement of the two types of octant (a) and (b). (e) Cation positions in spinel. Numbers refer to fractional heights, as multiples of $c/8$. Oxygens O′ are also shown in (b, c)

To complete the structure, we need to locate the tetrahedral A cations. In an *fcc* anion array, Fig. 1.20, the eight tetrahedral sites, 5-12, are located as shown. These tetrahedral sites are equidistant from oxygen atoms but also from the octahedral cation sites (e.g. distances 9-A and 9-3 in Fig. 1.20 are equal). Cation-cation repulsions do not allow adjacent tetrahedral and octahedral sites to be occupied simultaneously (this would be equivalent to tetrahedra and octahedra sharing a common face). We therefore need to find those tetrahedral sites for which all four neighbouring octahedral sites are empty. In Fig. 1.37(a), *all* of the tetrahedral sites (5-12 in Fig. 1.20) have at least one neighbouring octahedral cation and so none of the tetrahedral sites in this octant is occupied. The octant immediately below (or above) that in (a) is shown in (b); note that its top face is the same as the bottom face in (a). In this octant, two of the tetrahedral sites (positions 8 and 9 in Fig. 1.20) have no octahedral cation neighbours and therefore, both of these contain an A cation. Taking the spinel structure as a whole, the eight octants fall into two structural groups, as represented by (a) and (b). The A cations are located in the four octants of type (b).

The two types of octant are arranged such that they alternate in any of the three unit cell directions. They are, in fact, arranged in exactly the same way as anions and cations in the rock salt structure, Fig. 1.37(d). A projection of the unit cell onto one face, showing cation

positions only, is shown in (e). The orientation is exactly the same as in (b) and (c) but now atom heights, above the plane of the paper, are given as multiples of $c/8$. Octahedral positions are solid circles, occupied tetrahedral positions are represented by A. You should be able to see that the octahedral atoms O' i the base (height O) are the same as in (b, c).

We have given here a simplified description of the spinel structure. In practice, the a ions are displaced slightly from their corner and face centre positions. The degree of displacement varies slightly from compound to compound which does mean that the bond lengths to A and B cations can change so as to best fit those required by the particular A and B ions. The origin of the spinel structure is usually shifted to coincide with a tetrahedral A cation. We need not pursue this any further as it may lead to confusion, but it does lead to alternative descriptions of the spinel structure (e.g. the A cations alone are arranged in the same way as the C atoms in the diamond structure!)

A complicating factor in some spinel structures is that the cation distribution may vary. Two extreme types of behaviour may be distinguished. In spinels, the cations occupy sites given by the formula

$$[A]^{tet}[B_2]^{oct}O_4$$
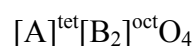
i.e. with A in tetrahedral sites and B in octahedral sites. Examples of normal spinels are $MgAl_2O_4$ and $MgTi_2O_4$. In *inverse* spinels, half of the B ions occupy tetrahedral sites, leaving the remaining B ions and all the A ions in octahedral sites, i.e.

$$[B]^{tet}[A,B]^{oct}O_4$$

Usually the cations A and B are disordered over the octahedral sites. Examples of inverse spinels are $MgFe_2O_4$ and Mg_2TiO_4.

As well as normal and inverse spinels, a complete range of intermediate cation distributions is possible and in some cases, the distribution changes with temperature. The cation distribution may be quantified using a parameter, γ, which is the fraction of A ions on the octahedral sites:
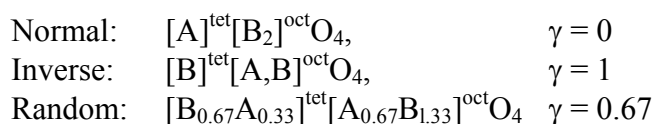
Normal: $[A]^{tet}[B_2]^{oct}O_4,$ $\gamma = 0$
Inverse: $[B]^{tet}[A,B]^{oct}O_4,$ $\gamma = 1$
Random: $[B_{0.67}A_{0.33}]^{tet}[A_{0.67}B_{1.33}]^{oct}O_4$ $\gamma = 0.67$

Table 1.20 *Some compounds with the spinel structure*

Compound	Type	$a(\text{Å})$	Structure	Compound	Type	$a(\text{Å})$	Structure
$MgAl_2O_4$	2, 3	8.0800	Normal	$MgIn_2O_4$	2, 3	8.81	Inverse
$CoAl_2O_4$	2, 3	8.1068	Normal	$MgIn_2S_4$	2, 3	10.708	Inverse
$CuCr_2S_4$	2, 3	9.629	Normal	Mg_2TiO_4	2, 4	8.44	Inverse
$CuCr_2Se_4$	2, 3	10.357	Normal	Zn_2SnO_4	2, 4	8.70	Inverse
$CuCr_2Te_4$	2, 3 ·	11.051	Normal	Zn_2TiO_4	2, 4	8.467	Inverse
$MgTi_2O_4$	2, 3	8.474	Normal	$LiAlTiO_4$	1, 3, 4	8.34	Li in tet
Co_2GeO_4	2, 4	8.318	Normal	$LiMnTiO_4$	1, 3, 4	8.30	Li in tet
Fe_2GeO_4	2, 4	8.411	Normal	$LiZnSbO_4$	1, 2, 5	8.55	Li in tet
$MgFe_2O_4$	2, 3	8.389	Inverse	$LiCoSbO_4$	1, 2, 5	8.56	Li in tet
$NiFe_2O_4$	2, 3	8.3532	Inverse				

The cation distribution in spinels and the *degree of inversion, γ,* have been studied in considerable detail. Several factors influence γ, including the site preferences of ions in terms

of size, covalent bonding effects and crystal field stabilization energies (Chapter 2). The γ value in any particular spinel is given by the net effect of these various parameters taken together. Some compounds with the spinel structure are given in Table 1.20.

j) Silicate structures-some tips to understanding them

Silicates, especially many minerals, often have complex formulae and structures. The purpose of this section is not to give a review of their structures but simply to show that a considerable amount of structural information may be obtained from their chemical formulae. Using certain guidelines one can appreciate, without the necessity of remembering a large number of complex formulae, whether a particular silicate is a 3D framework structure, sheet-like, chain-like, etc.

It is common practice to regard silicate structures as composed of cations and silicate anions. Various silicate anions are possible, ranging from the extremes of isolated SiO_4^{4-} tetrahedra in orthosilicates such as olivine (Mg_2SiO_4), to infinite 3D frameworks, as in silica itself (SiO_2). The structures of silicate anions are based on certain principles:

(1) Almost all silicate structures are built of SiO_4 tetrahedra.
(2) The tetrahedra link by sharing corners to form larger polymeric units.
(3) No more than two SiO_4 tetrahedra may share a common corner (i.e. oxygen).
(4) SiO_4 tetrahedra never share edges or faces with each other.

Exceptions to (1) are structures in which Si is octahedrally coordinated to O as in one polymorph of SiP_2O_7 and in high pressure polymorphs of SiO_2 (coesite, stishovite). The number of these exceptions is very small, however, and we can regard SiO_4 tetrahedra as the normal building block in silicate structures. Guidelines (3) and (4) are concerned respectively with maintaining local electroneutrality and with ensuring that highly charged cations, such as Si^{4+}, are not too close together.
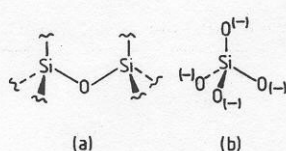

Fig. 1.38 Silicate anions with (a) bridging and (b) non-bridging oxygens

The important factor in relating formula to structure type is the Si:O ratio. This ratio is variable since two types of O may be distinguished in the silicate anions: *bridging oxygens* and *non-bridging oxygens*. Bridging oxygens are those that link two tetrahedra, Fig. 1.38(a). Effectively, they belong half to one Si and half to another Si. In evaluating the net Si:O ratio, bridging oxygens count as ½. Non-bridging oxygens are linked to only one Si or silicate tetrahedron as in (b). They are also called terminal oxygens. In order to maintain charge balance, non-bridging oxygens must of course also be linked to other cations in the crystal structure. In evaluating the overall Si:O ratio, non-bridging oxygens count as 1.

The overall Si:O ratio in a silicate structure depends on the relative number of bridging and non-bridging oxygens. Some examples are given in Table 1.21; they are all straightforward and one may deduce the type of silicate anion directly from the chemical formula.

Many more complex examples could be given. In these, although the detailed structure cannot be deduced from the formula, one can at least get an approximate idea of the type of silicate anion. For example, in $Na_2Si_3O_7$, the Si:O ratio is 1:2.33. This corresponds to a

structure in which, on average, two-thirds of an O per SiO_4 is non-bridging. Clearly, therefore, some $SiO4$ tetrahedra must be composed entirely of bridging oxygens whereas others contain one non-bridging oxygen. The structure of the silicate anion would therefore be expected to be something between an infinite sheet and a 3D framework. In fact, it is an infinite, double-sheet silicate anion in which two-thirds of the silicate tetrahedra have one non-bridging O.

Table 1.21 *Relation between chemical formula and silicate anion structure*

Si:O ratio	Number of oxygens per Si		Type of silicate anion	Examples
	bridging	non-bridging		
1:4	0	4	isolated SiO_4^{4-}	Mg_2SiO_4 olivine, Li_4SiO_4
1:3.5	1	3	dimer $Si_2O_7^{6-}$	$Ca_3Si_2O_7$ rankinite, $Sc_2Si_2O_7$ thortveite
1:3	2	2	chains $(SiO_3)_n^{2n-}$	Na_2SiO_3, $MgSiO_3$ pyroxene
			rings, e.g. $Si_3O_9^{6-}$	$CaSiO_3^*$, $BaTiSi_3O_9$ benitoite
			$Si_6O_{18}^{12-}$	$Be_3Al_2Si_6O_{18}$ beryl
1:2.5	3	1	sheets $(Si_2O_5)_n^{2n-}$	$Na_2Si_2O_5$
1:2	4	0	3D framework	$SiO_2^\dagger$

* $CaSiO_3$ is dimorphic. One polymorph has $Si_3O_9^{6-}$ rings. The other polymorph has infinite $(SiO_3)_n^{2n-}$ chains.
† The three main polymorphs of silica: quartz, tridymite and cristobalite each have a different kind of 3D framework structure.

The relation between formula and anion structure is more complex when Al is present.

In some cases, Al substitutes for Si, in the tetrahedra; in others, it occupies octahedral sites. In the plagioclase feldspars typified by albite, $NaAlSi_3O_8$ and anorthite, $CaAl_2Si_2O_8$, Al partly replaces Si in the silicate anion. It is therefore appropriate to consider the overall ratio (Si + Al) : O. In both cases, this ratio is 1:2 and therefore, a 3D framework structure is expected. Framework structures also occur in orthoclase, $KAlSi_3O_8$, kalsilite, $KAlSiO_4$, eucryptite, $LiAlSiO_4$ and spodumene, $LiAlSi_2O_6$.

Substitution of Al for Si occurs in many sheet structures such as micas and clay minerals. Talc has the formula, $Mg_3(OH)_2Si_4O_{10}$ and, as expected for an Si:O ratio of 1:2.5, the structure contains infinite silicate sheets. In the mica phlogopite, one quarter of the Si in talc is effectively replaced by Al and extra K is added to preserve electroneutrality. Hence, phlogopite has the formula $KMg_3(OH)_2(Si_3Al)O_{10}$. In talc and phlogopite, Mg occupies octahedral sites between silicate sheets; K occupies 12-coordinate sites. The mica muscovite, $KAl_2(OH)_2(Si_3Al)O_{10}$ is more complex; it is structurally similar to phlogopite, with infinite sheets, $(Si_3Al)O_{10}$. However, two other Al^{3+} ions replace the three Mg^{2+} ions of phlogopite and occupy octahedral sites. By convention, only ions that replace Si in tetrahedral sites are included as part of the complex anion. Hence octahedral Al^{3+} ions are formally regarded as cations in much the same way as alkali and alkaline earth cations, Table 1.21.

With a few exceptions, silicate structures cannot be described as *cp*. However, this disadvantage is offset by the clear identification of the silicate anion component which facilitates classification and description of a very wide range of structures. In addition, the Si-O bond is strong and partially covalent and the consequent stability of the silicate anion is responsible for many of the properties of silicates.

Table 1.4 *Some close packed structures*

Anion arrangement	Interstitial sites			Examples
	T_+	T_-	O	
ccp	—	—	1	NaCl, rock salt
	1	—	—	ZnS, blende or sphalerite
	$\frac{1}{8}$	$\frac{1}{8}$	$\frac{1}{2}$	$MgAl_2O_4$, spinel
	—	—	$\frac{1}{2}$	$CdCl_2$
	—	—	$\frac{1}{3}$	$CrCl_3$
	1	1	—	K_2O, antifluorite
hcp	—	—	1	NiAs
	1	—	—	ZnS, wurtzite
	—	—	$\frac{1}{2}$	CdI_2
	—	—	$\frac{1}{2}$	TiO_2, rutile*
	—	—	$\frac{2}{3}$	Al_2O_3, corundum
	$\frac{1}{8}$	$\frac{1}{8}$	$\frac{1}{2}$	Mg_2SiO_4, olivine
ccp 'BaO$_3$' layers	—	—	$\frac{1}{4}$	$BaTiO_3$, perovskite

* The *hcp* oxide layers in rutile are not planar but are buckled; the oxide ion arrangement may alternatively be described as *tetragonal packed* (*tp*).